MODELING AND SIMULATION OF A STEAM POWER STATION

by

ALBERTO AZUMA

B. S., ESCOLA POLITECNICA DA UNIVERSIDADE DE S. PAULO
(1963)

SUBMITTED IN PARTIAL FULFILLMENT
OF THE REQUIREMENTS FOR THE
DEGREE OF

MASTER OF SCIENCE IN MECHANICAL ENGINEERING

at the

MASSACHUSETTS INSTITUTE OF TECHNOLOGY

AUGUST, 1975

Signature of Author . . . . . .
Department of Mechanical Engineering, August 11, 1975

Certified by . . . . . .
Thesis Supervisor

Accepted by . . . . . .
Chairman, Department Committee on Graduate Students

MODELING AND SIMULATION OF A STEAM POWER STATION

by

ALBERTO AZUMA

Submitted to the Department of Mechanical Engineering on August 11, 1975, in partial fulfillment of the requirements for the Degree of Master of Science in Mechanical Engineering.

ABSTRACT

A fifth-order turbine-governor and a third-order oil-firing boiler model for a steam power plant are developed and combined into a complete plant model. A classical PID controller and an Optimal Integral Controller are applied to the plant model, and the results are compared for two different load levels and different kinds of disturbances. Special attention is given to the turbine throttle pressure behaviour and to the overshoot in firing intensity following the disturbances. The suitability of Optimal Integral Controller has been demonstrated.

The final model and control system can be used for dynamic stability studies of large interconnected systems.

Thesis Supervisor: Professor D. N. Wormley
Title: Associate Professor of Mechanical Engineering

ACKNOWLEDGMENTS

The author is indebted to his advisor, Professor D. N. Wormley, for his guidance and encouragement during the progress of this work; to Professor H. M. Paynter whose interest and valuable suggestions were decisive to its successful completion; and to Mr. G. Masada for the basic plant information and useful discussions during the development of the model and controls.

The author wishes to express his gratitude to Light-Servicos de Eletricidade S/A who supported his graduate work.

Finally, the author also wishes to acknowledge his gratitude to his wife, Irene, for her patience and moral support given during this academic period.

TABLE OF CONTENTS

LIST OF TABLES

LIST OF FIGURES

LIST OF COMPUTER PROGRAMS

I. INTRODUCTION

Mathematical models of steam power plants have been developed by several researchers, mainly for purposes of dynamic stability analysis of interconnected electrical systems.

For the study of short transients, i.e., limited to a few seconds, one would need only a simplified model of the turbine-generator set and its associated speed and voltage regulators. In such cases the boiler acts as a source of constant pressure due to its large accumulation capacity, even considering the modern fast-response, once-through type boilers.

In the case considered in this thesis which includes the load response to a step change in control valve position, a simple model may not be adequate, and a more detailed representation must be used for the turbine and boiler.

On this study a low-order model is developed for a drum-type oil-firing boiler coupled to a more detailed turbine model, in order to make the final model suitable for stability studies of interconnected systems. The main concern with the boiler is to obtain a good pressure response by adequate selection of the combustion controller type.

A digital computer program simulation is developed so that different drum-type boilers and single reheat turbines can be modeled by appropriate change of the parameters by merely changing the input data cards. The program also allows one to obtain the eigenvalues of the system as a direct output.

II. MODEL OF THE PLANT

II.1 The Boiler Model

II.1.1 General

The boiler incorporates a relatively large number of equipment: fuel and water pumps, draft fans, burners, heat exchangers, and so on. The modeling of the effects of each component into a global model is impractical, and the resulting order of the system would be out of hand. Thus, in practice, depending upon the purpose of study, one tries to obtain a simplified model capable of simulating the most important effects. The degree of detail of such a model varies in a broad range, even for control purposes. In the case where a suitable control for a particular boiler is desired, we would have to model the effects of internal couplings in a reasonable detail, and precise knowledge of design characteristics of the boiler would be required. On the other hand, if the purpose of study is to analyse the general behaviour of a certain type of boiler under different control schemes, then a more general and less detailed model could be suitable. Our task is more closely related to this last case.

Of course, one could point out that to conveniently represent an actual boiler by means of a low-order model, we would have to start from a detailed model and make the necessary simplifications. However, such a procedure is usually a difficult task [7] as each reduction involves some assumptions as to what can be safely neglected, i.e., without distorting the boiler characteristics. Some techniques are available for reduction [17] of high-order systems.

The available literature [6,7,8,9,12] has provided several examples of low-order linear models for boilers. Such models can reasonably represent the response of certain physical variables of interest within small deviations about a certain operating point. Most of such models are variations of the model originally proposed by Profos [2] resulting in different but basically equivalent models suitable for our purpose. In general, the variable of interest is the main steam pressure, herein after designated as "throttle" pressure. The importance of the pressure control is well known as the main link between the separate boiler and turbine controls in the "boiler follow" model of operation, and this task is performed by the combustion controller, or "boiler master control."

II.1.2 Boiler Model Components

The basic model proposed by Profos [2] is shown in Fig. 1.

The firing system consists of two interconnected subsystems--the fuel flow control and air flow control which maintains a suitable air/fuel ratio. The output of interest in this case is the fuel flow, but it can be translated in terms of fuel oil pressure. We will refer to the rate of fuel supply and burning as "firing intensity" (F) and to the control signal to the firing system as "firing setting" (C_F). The oil firing system can be represented by a simple lag [2] as illustrated in Fig. 2. The value of the time constant T_F is evaluated in Appendix I.

Part of the heat released by combustion of supplied fuel is transferred to the water in the waterwall raiser tubes to convert it into steam. Most of the heat transfer is made by radiation, and the time

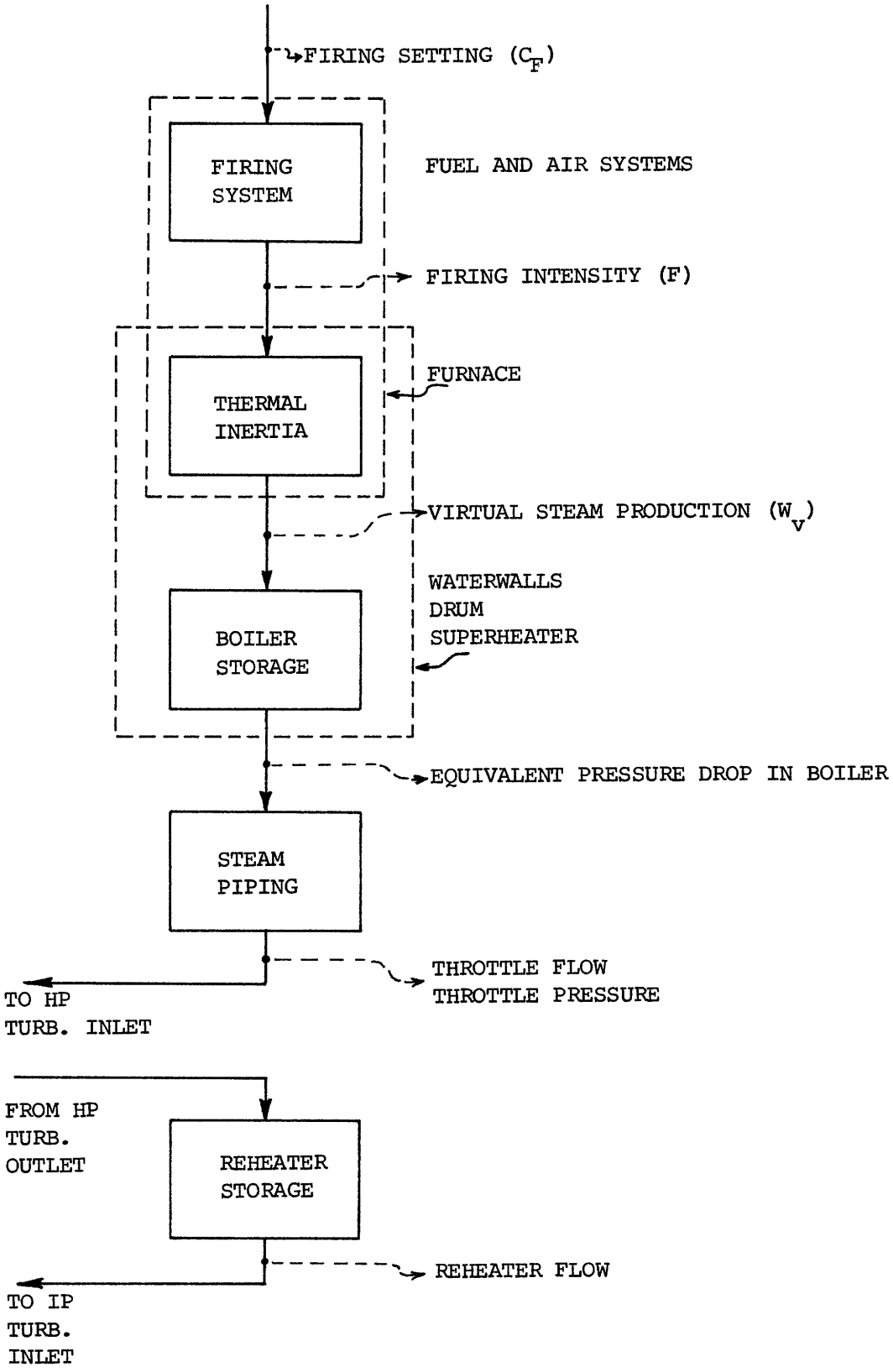

Fig. 1. Profo's Boiler Model

constant associated with this process can be neglected [1] in comparison with the much larger time constant involved in the storage capacity of the boiler. Considering that the water in the raiser tubes is at the saturation temperature corresponding to the boiler pressure, any additional heat transferred to it is immediately converted into steam. This steam production at constant pressure due to the heat transfer is called "virtual steam production" (W_v). In general, it is represented as a simple lag as in Fig. 3, where, in our case, the time constant T_v is negligible ($T_v \simeq 0$).

When boiler pressure decreases, as in the case of a load increase (increase in steam flow), then an additional steam production takes place due to the change in the equilibrium temperature of the saturated water in the raiser tubes and drum [1], corresponding to a process also known as "flashing steam" production. The decrease in saturation temperature takes place immediately as pressure decreases, and the heated walls of the raiser tubes and drum transfer part of the stored thermal energy in order to reach the new equilibrium point. Such process is independent of the heat input rate from combustion and helps prevent a rapid decrease in the boiler pressure as steam demand suddenly increases. Its effect is added to the mass accumulation capacity of the steam space at the drum and superheater, and it can be represented by a single capacitance as in Fig. 4.

In Appendix I we present the details for the calculation of the storage time constant TR. The rate of change of steam quantity in boiler corresponds to the difference between the virtual steam production and the rate of steam take-off from the drum. Note that we are

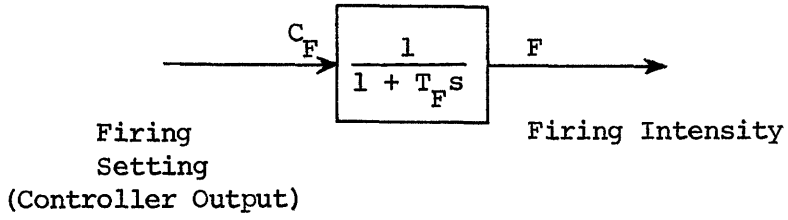

Fig. 2 Firing System

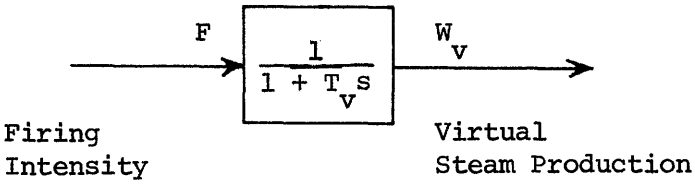

Fig. 3 Thermal Inertia

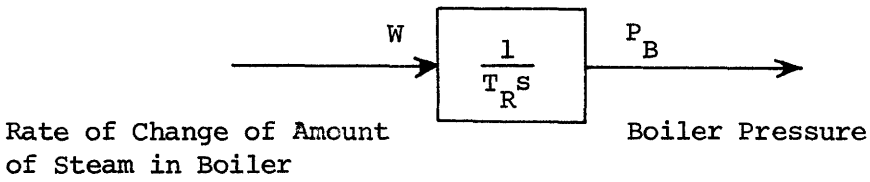

Fig. 4 Accumulation Capacity of Boiler

assuming a constant volume of the steam space in the boiler, and this presupposes the existence of an ideal feedwater flow controller which is not a too strong assumption [6] considering the purpose of our model. Small variations in water level in the drum will not sensibly affect the value of T_R.

The pressure drop through the steam path following the boiler drum is lumped into an equivalent total pressure drop between the drum and the turbine throttle. The storage capacity of the main steam piping is taken into account in order to include its effects in the initial throttle pressure transients following a change in steam consumption although the time constant associated with the piping (T_P) is relatively small.

The boiler storage, piping storage, and pressure drop can be represented by the bond graph in Fig. 5.

From the bond graph one can derive the following governing equations:

$$\dot{P}_B = \frac{1}{T_R} (W_V - W_{SH}) \tag{1}$$

where $W_V - W_{SH} = W$, the rate of change of amount of steam in boiler as mentioned previously;

$$\dot{P}_T = \frac{1}{T_P} (W_{SH} - W_o) \tag{2}$$

where W_o = throttle flow;

$$W_{SH} = K_{SH}(P_B - P_T) \tag{3}$$

where K_{SH} represents the equivalent linear conductance of the steam path, which replaces the quadratic law resistance within small deviations from the operating point.

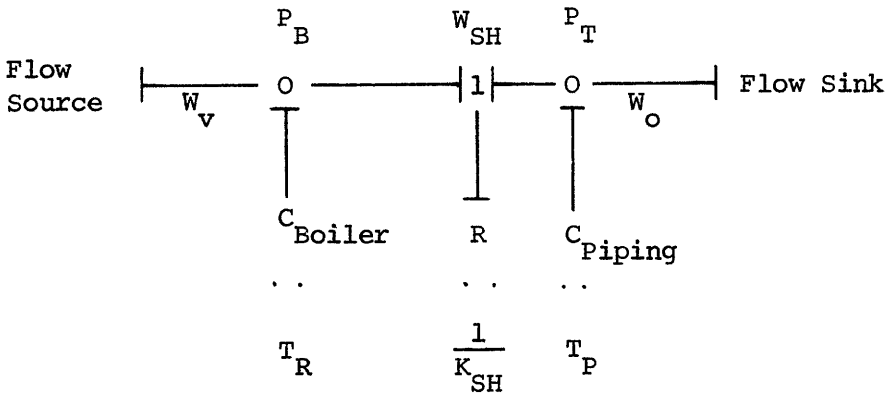

Fig. 5 Bond Graph for Boiler Storage and Pressure Drop

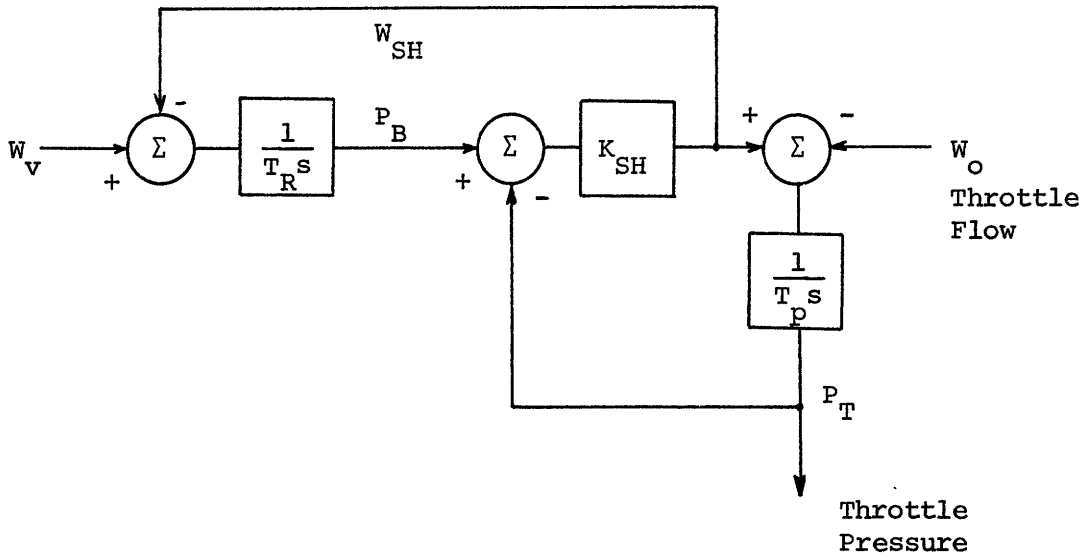

Fig. 6 Block Diagram for Storage Capacity and Pressure Drop

The block diagram of boiler storage and pressure drop is shown in Fig. 6.

The "throttle flow" corresponds to the flow through the turbine control valves, and it depends not only on the throttle pressure but also on the valve stroke which in its turn depends on the turbine load and speed conditions. We have reached, thus, the coupling region between the boiler and the turbine.

The computation of the parameters of the boiler and turbine is presented in Appendix II, and the results for the boiler is shown in Table 1. The complete boiler model is third order.

II.1.3 The Final Boiler Model

Parameter	Load Level	
	90%	60%
T_F	10 sec	10 sec
T_R	127 sec	242 sec
K_{SH}	20	59
T_P	1.5 sec	3.0 sec

Table 1 - Boiler Parameters

The complete boiler model is shown in Fig. 7, together with a classical control configuration.

II.2 The Turbine Model

II.2.1 General

We present a more detailed model for the turbine-governor system than that for the boiler, and this fact is justified by the purpose of

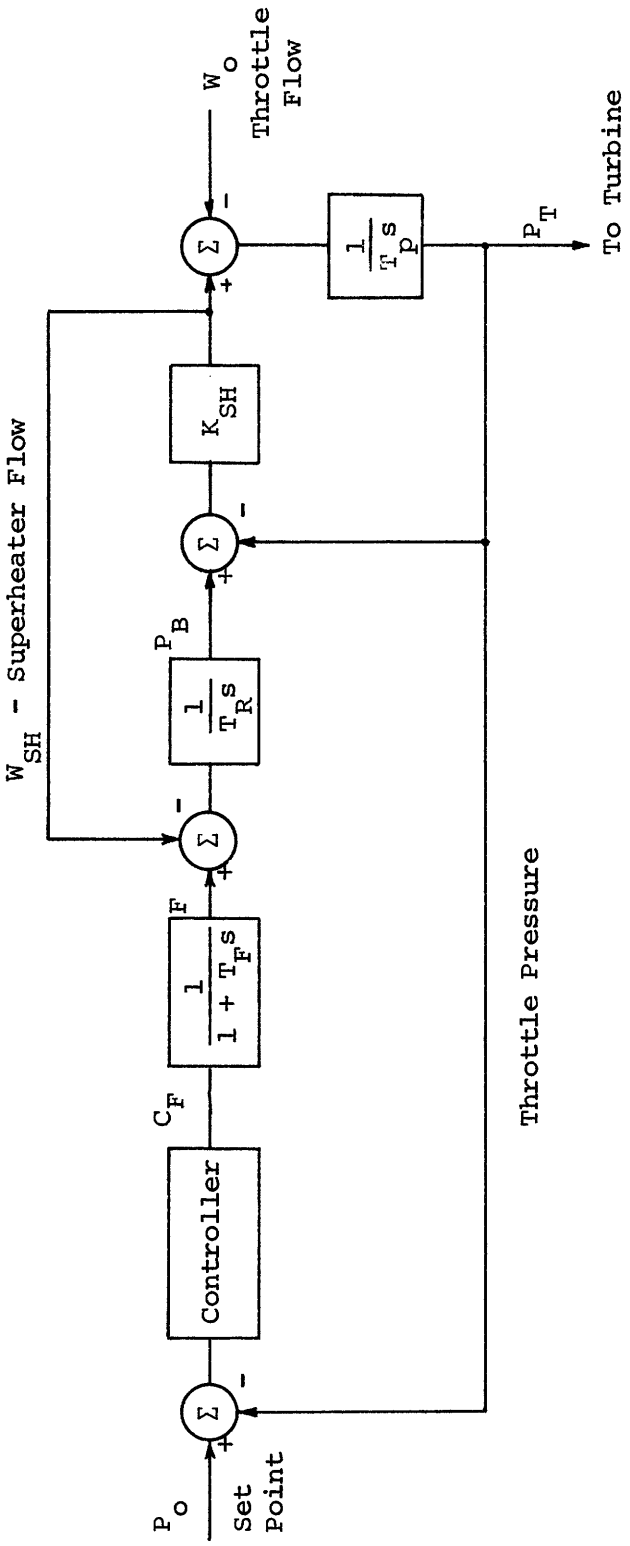

Fig. 7 Boiler Model with Classical Control

study as explained in Chapter I. There are many available publications dealing with turbine models for large-scale stability studies applied to electrical interconnected systems [11,12]. We based our model on the work of T. L. Shang [13], with some modifications and the inclusion of a low-pressure turbine separated from the intermediate pressure turbine by a "crossover" piping. Some basic numerical values for parameters were obtained from the Boston Edison, Mystic No. 4 simulation model (see Appendix II-b), and some unavailable data were estimated based on typical values for large turbines.

The electrical generator is considered a part of the environment, and its effect is taken into account by means of a "frequency-load" (damping) characteristic factor, θ [6,9].

II.2.2 Turbine Model Development

A tandem-compound tripple-flow turbine with one reheat system can be represented by a bond graph [13] as in Fig. 8(b), corresponding to the physical arrangement of Fig. 8(a).

Control Valves:

We suppose that the steam is supplied at pressure P_T at the turbine control valves. The flow through the valves depends on such pressure, on the equivalent valve stroke, z, and on the valves back-pressure p_1, which corresponds to the steam pressure to the turbine first stage:

$$W_o = W_o(p_T, p_1, z) \tag{4}$$

$$dW_o = \underbrace{\frac{\partial W_o}{\partial p_T}}_{\xi} dp_T + \underbrace{\frac{\partial W_o}{\partial p_1}}_{\beta} dp_1 + \frac{\partial W_o}{\partial z} dz \quad . \tag{5}$$

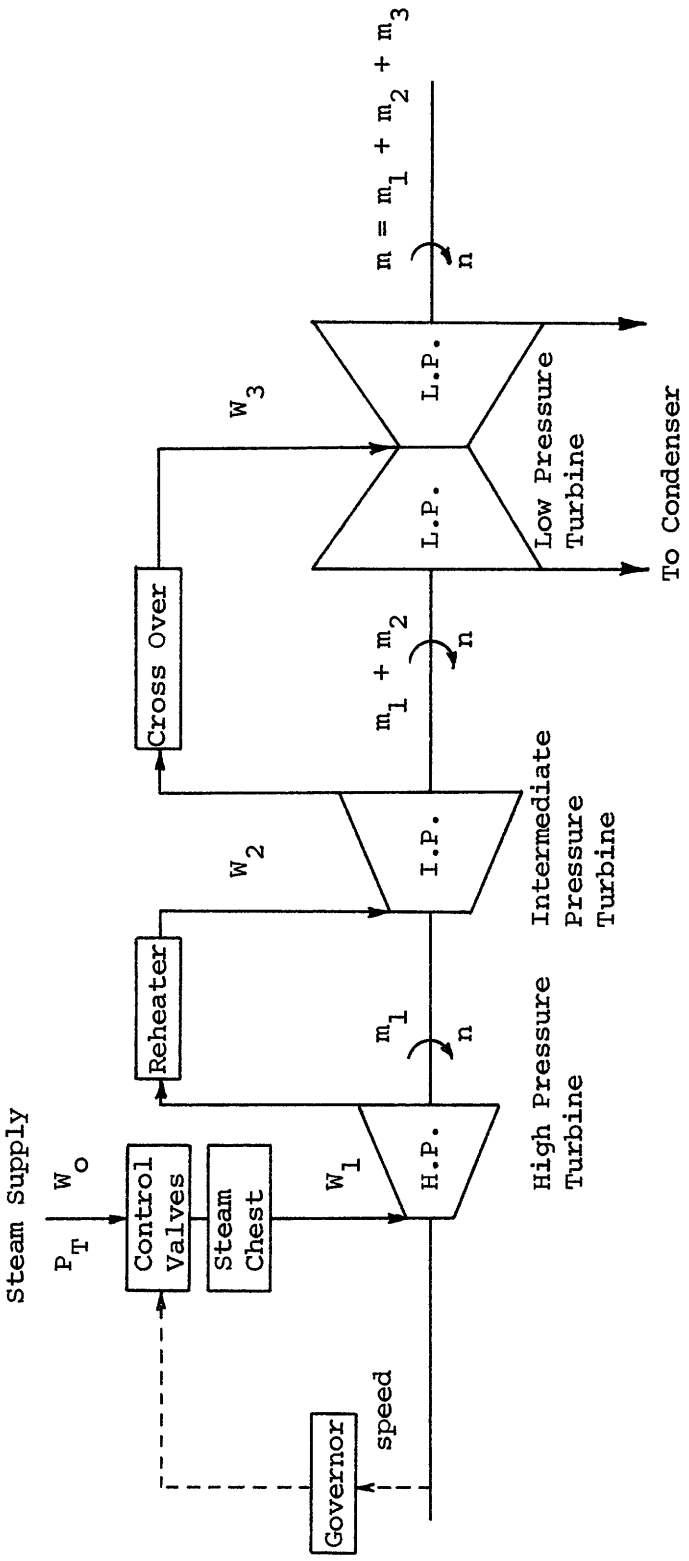

Fig. 8(a) Physical Arrangement

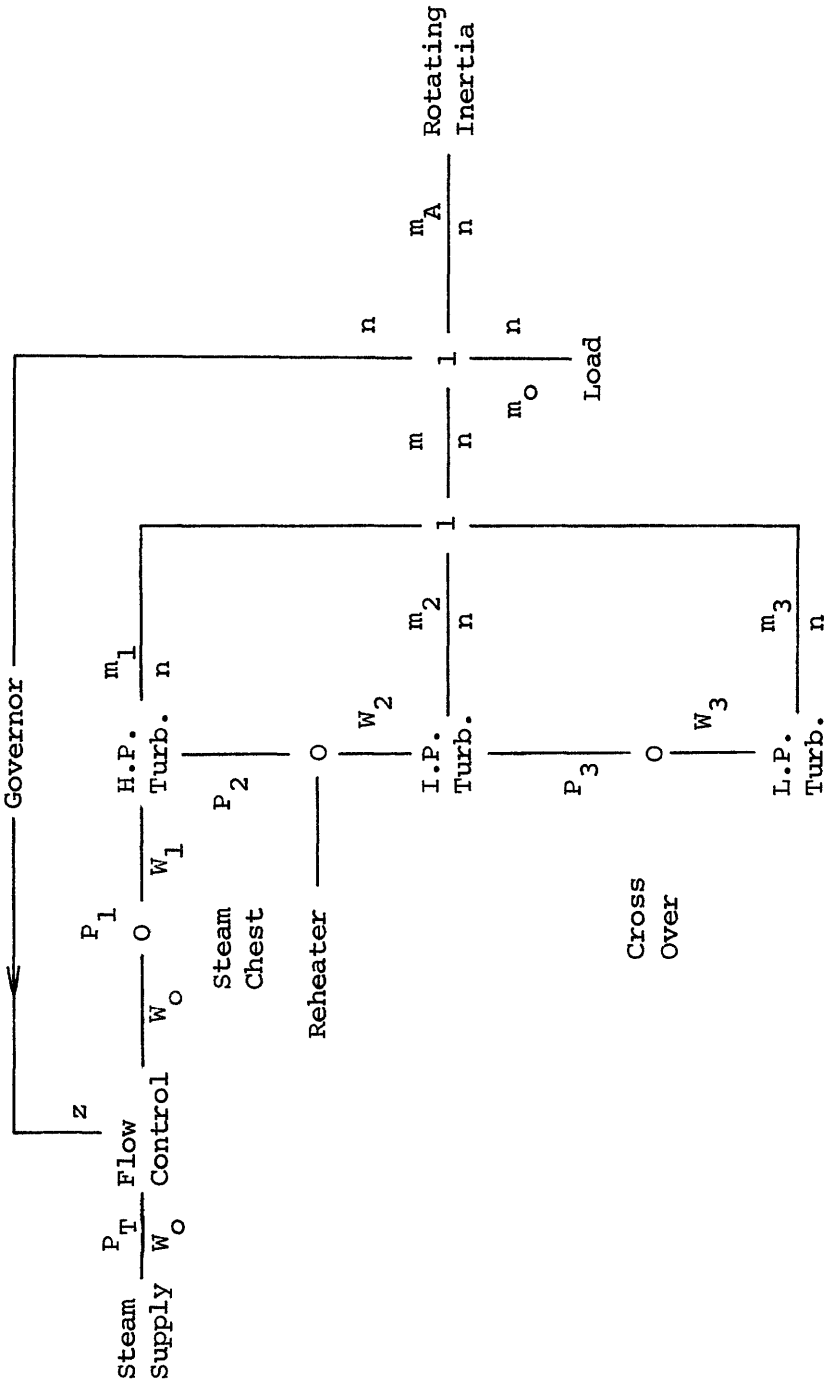

Fig. 8(b) Bond Graph

In terms of linear, per-unit increment form, we can write:

$$W_o = \xi p_T + \beta p_1 + z \tag{6}$$

where W_o, p_T, p_1, and z now represent the per-unit deviations about a steady-state operating point. The value of z includes the partial derivative $\frac{\partial W_o}{\partial z}$ in the sense that the characteristics of control values can be designed to be linear. In the case of chocked flow, $\beta = o$, but even in the case of non-chocked flow, the design characteristic of the control valves can include such effects in order to make W_o independent of p_1.

In our equations we keep the form (6), allowing one to include any value of the parameters ξ and β.

Steam Chest:

The steam chest corresponds to the steam accumulation capacitance between the control valves and the high pressure first stage of the turbine. It is usually represented as a first-order lag [11] as follows:

$$p_1 = \frac{1}{T_{CH}s} \quad (W_o - W_1) \tag{7}$$

where T_{CH} is the steam chest time constant and p_1 the steam pressure to the first stage.

The flow to the first stage depends on p_1 and the back pressure p_2. However, p_2 is usually the critical pressure such that in linear, per-unit form we can write

$$W_1 \equiv p_1 \ ; \tag{8}$$

that is, the increment in steam flow to the first stage is numerically equal to the increment in stage pressure.

Thus,

$$W_1 = p_1 = \frac{1}{1 + T_{CH}s} W_o \ . \tag{9}$$

The coupling region between the boiler and turbine can thus be represented in a block diagram as in Fig. 9.

Reheater and Cross-Over:

By similar reasoning we can write

$$W_2 = \frac{1}{1 + T_{RH}s} W_1 \tag{10}$$

$$W_3 = \frac{1}{1 + T_{CO}s} W_2 \tag{11}$$

where W_2, W_3 are the steam flows to the I.P. and L.P. turbine, respectively, and T_{RH}, T_{CO} are the time constant associated with the mass storage capacity of reheater and cross-over, respectively. Notice that T_{RH} must include also the storage capacity of steam pipes between the turbine and the reheater.

The pressure drop in the reheater is usually small because the gain in efficiency by the use of reheat could be impaired by a too large energy loss by friction. In our model we neglect pressure drops in reheater and in the cross-over.

High Pressure Turbine:

The turbine output torque can be expressed as a function of the isentropic enthalpy drop, steam flow, and speed as follows:

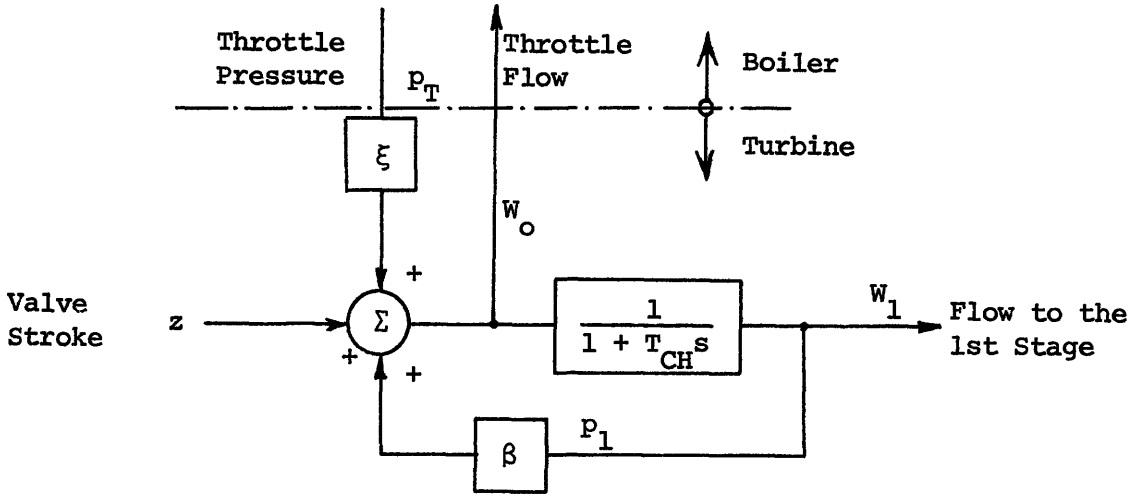

Fig. 9 Coupling Between Boiler and Turbine

$$M_1 = \frac{H_1 W_1}{N} \cdot \eta \tag{12}$$

where H_1, W_1, and N are the enthalpy drop, flow and speed, respectively. η represents the internal efficiency of the turbine, which is assumed constant during small load excursions.

In terms of incremental values we can write:

$$dM_1 = \frac{\partial H_1}{\partial H_1} dH_1 + \frac{\partial H_1}{\partial W_1} dW_1 + \frac{\partial H_1}{\partial N} dN \tag{13}$$

$$= \frac{\eta}{N} W_1 dH_1 + \frac{\eta}{N} H_1 dW_1 + \eta(-\frac{1}{N^2}) H_1 W_1 dN \quad . \tag{14}$$

To obtain the torque as per-unit increment based on steady state H.P. turbine torque, we divide such expression by M_{10} (steady-state value) to obtain:

$$m_1' = h_I - W_1 - n \tag{15}$$

where

$$h_I = \frac{dH_1}{H_{10}} \quad , \tag{16}$$

$$W_1 = \frac{dW_1}{W_{10}} \quad , \tag{17}$$

$$n = \frac{dN}{N_o} \quad , \tag{18}$$

and where H_{10} represents the enthalpy drop in the H.P. turbine at steady state conditions

If f_{HP} is the power fraction of the H.P. turbine, i.e., that portion of the total power obtained from the H.P. turbine, then the torque contribution corresponding to it can be written as follows, provided that the speed N_o is the same for all stages:

$$m_1 = f_{HP}\, m_1' = f_{HP}(h_I + W_1 - n) \tag{19}$$

But $$h_I = \frac{\partial h_I}{\partial p_1}\, p_1 + \frac{\partial h_I}{\partial p_2}\, p_2 \tag{20}$$

$$m_1 = f_{HP}\left(\frac{\partial h_I}{\partial p_1}\, p_1 + \frac{\partial h_I}{\partial p_2}\, p_2 + W_1 - n\right) . \tag{21}$$

Similarly, for the I.P. turbine, neglecting the pressure drop in the reheater, we get:

$$m_2 = f_{IP}\left(\frac{\partial h_{II}}{\partial p_2}\, p_2 + \frac{\partial h_{II}}{\partial p_3}\, p_3 - n\right) \tag{22}$$

where f_{IP} is the power fraction of the I.P. turbine and

$$h_{II} = \frac{\partial H_2}{H_{20}} = \frac{\text{incremental change in I.P. enthalpy drop}}{\text{steady-state enthalpy drop in I.P. turbine}} \tag{23}$$

For the L.P turbine, neglecting pressure drop in the cross-over piping, we have:

$$m_3 = f_{LP}\left(\frac{\partial h_{III}}{\partial p_3}\, p_3 + \frac{\partial h_{III}}{\partial p_f}\, p_f - n\right) \tag{24}$$

where f_{LP} is the power fraction of the L.P. turbine, $f_{LP} = 1 - f_{HP} - f_{IP}$, and

$$h_{III} = \frac{\partial H_3}{H_{30}} \quad ; \tag{25}$$

and where p_f is the incremental pressure at the L.P. turbine exhaust, i.e., the condenser pressure. As the condenser pressure can be assumed constant during small load swings, $p_f = 0$.

The total torque is the sum of the contributions of each turbine as follows:

$$m = f_{HP}\left(\frac{\partial h_I}{\partial p_1} p_1 + \frac{\partial h_I}{\partial p_2} p_2 + W_1 - n\right) +$$

$$+ f_{IP}\left(\frac{\partial h_{II}}{\partial p_2} p_2 + \frac{\partial h_{II}}{\partial p_3} p_3 + W_2 - n\right) + \qquad (26)$$

$$+ f_{LP}\left(\frac{\partial h_{III}}{\partial p_3} p_3 + W_3 - n\right) \quad .$$

To simplify the preceding expression, we will base on Fig. 10 and the following developments:

$$h_I = \frac{dH_1}{H_{10}} = \frac{d(H_I - H_{II})}{H_{10}} \qquad (27)$$

$$h_{II} = \frac{dH_2}{H_{20}} = \frac{d(H_{II}' - H_{III})}{H_{20}} = \frac{d[(H_I - H_{II}) + (H_{II}' - H_{III}) - (H_I - H_{II})]}{H_{20}} \qquad (28)$$

$$h_{II} = \frac{dH_1 + dH_2}{H_{20}} - h_I \frac{f_{HP}}{f_{IP}} \quad . \qquad (29)$$

A change in reheater pressure p_2 alone does not change the total increment $dH_1 + dH_2$; i.e., the extreme points I and III are unchanged. Thus,

$$\frac{\partial h_{II}}{\partial p_2} = - \frac{f_{HP}}{f_{IP}} \frac{\partial h_I}{\partial p_2} \quad . \qquad (30)$$

Similarly:

$$h_{III} = \frac{dH_3}{H_{30}} = \frac{d(H_{III} - H_{IV})}{H_{30}} = \frac{d[(H_{II}' - H_{III}) + (H_{III} - H_{IV}) - (H_{II}' - H_{III})]}{H_{30}} \qquad (31)$$

$$h_{III} = \frac{dH_2 + dH_3}{H_{30}} - h_{II} \frac{f_{IP}}{f_{LP}} \qquad (32)$$

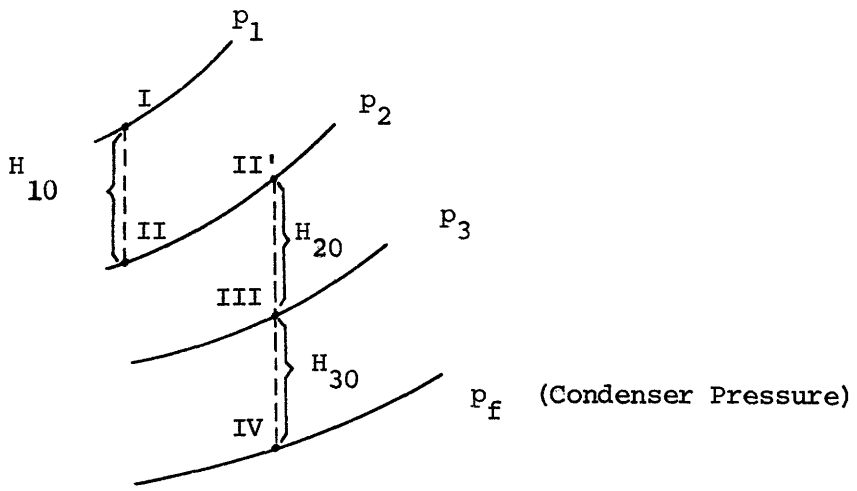

Fig. 10 Schematic Isentropic Enthalpy Drop

$$\frac{\partial h_{III}}{\partial p_3} = - \frac{f_{IP}}{f_{LP}} \frac{\partial h_{II}}{\partial p_3} \tag{33}$$

The equation for the total torque then become:

$$m = f_{HP} \frac{\partial h_I}{\partial p_1} p_1 + f_{HP} W_1 + f_{IP} W_2 + f_{LP} W_3 - n \tag{34}$$

or, as $W_1 \equiv p_1$, and making $\frac{\partial h_I}{\partial p_1} = \gamma$ (35)

$$m = f_{HP}(1 + \gamma) W_1 + f_{IP} W_2 + f_{LP} W_3 - n \tag{36}$$

The influence of speed in the total torque depends on the type of load connected to the output shaft. We can model the load by means of a "load-frequency" (damping) characteristic . The final equation thus becomes

$$m = f_{HP}(1 + \gamma) W_1 + f_{IP} W_2 + f_{LP} W_3 - \theta n \tag{37}$$

The corresponding block diagram is shown in Fig. 11.

The turbine parameters are evaluated in Appendix II-b, and the results are presented in Table 2.

Parameter	Load Level	
	90%	60%
ξ	1.0	1.0
β	0.0	0.0
γ	0.46	0.20
θ	0.0	0.0
T_{CH}	0.3	0.3
T_{RH}	3.3	3.0
T_{CO}	0.4	0.4
F_{HP}	0.3	0.4
F_{IP}	0.4	0.4
F_{LP}	0.3	0.2

Table 2 Turbine Parameters

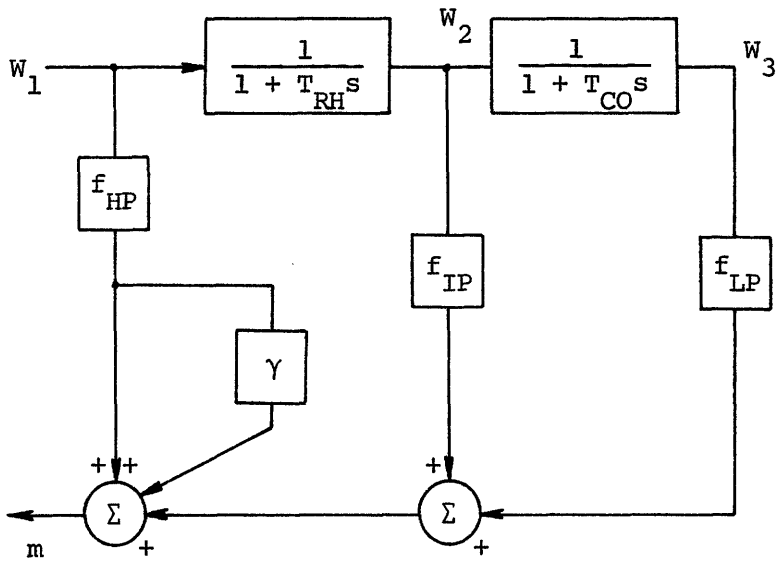

Fig. 11 Block Diagram of Turbine

II.2.3 The Governor Model

Several models for the speed governor have been proposed in the available literature [11,12,13]. For simplicity, we adopted the model used by Shang [19] which consists in the following components (Fig. 12):

$\frac{K}{\delta}$ - represents the governor gain. We assumed K = 1 and δ, the speed droop, as 6% [11].

T_{SV} - is the servomotor time constant, assumed equal to 0.3 sec [13].

T_A - is the rotor inertia time, assumed to be equal to 10 sec [6].

II.3 The Plant Model

Combining the boiler and the turbine-governor models, we obtain the eight-order plant model as illustrated in Fig. 13.

The eigenvalues of the plant system are presented in Table 3.

Real Part	Imaginary Part
- 14.15	--
- 4.609	--
- 2.065	+ j 0.4187
- 2.065	- j 0.4187
- 0.367	+ j 0.7823
- 0.367	- j 0.7823
- 0.100	--
- 0.0000384	--

Table 3 Eigenvalues of Open-loop System at 90% Load Level

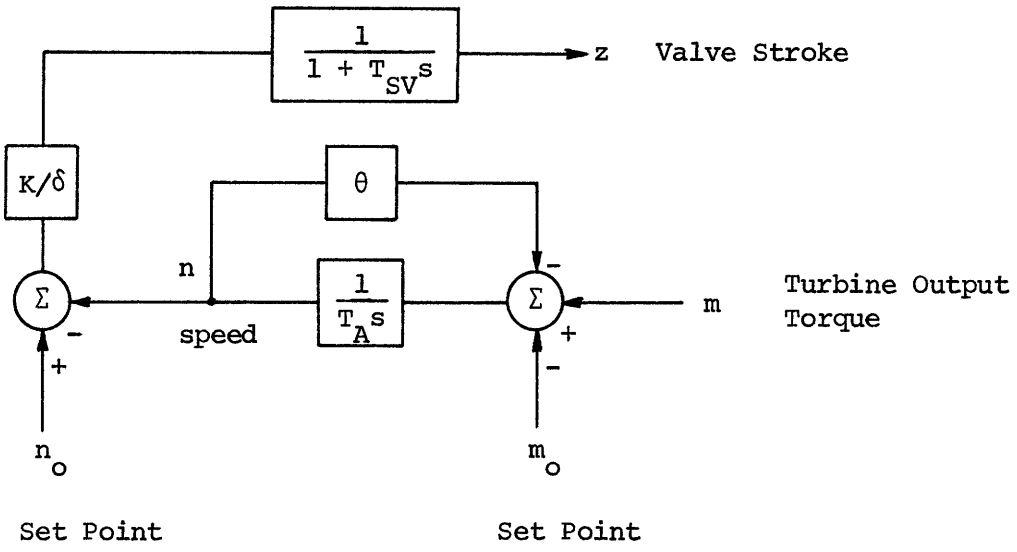

Fig. 12 Speed Governor Representation

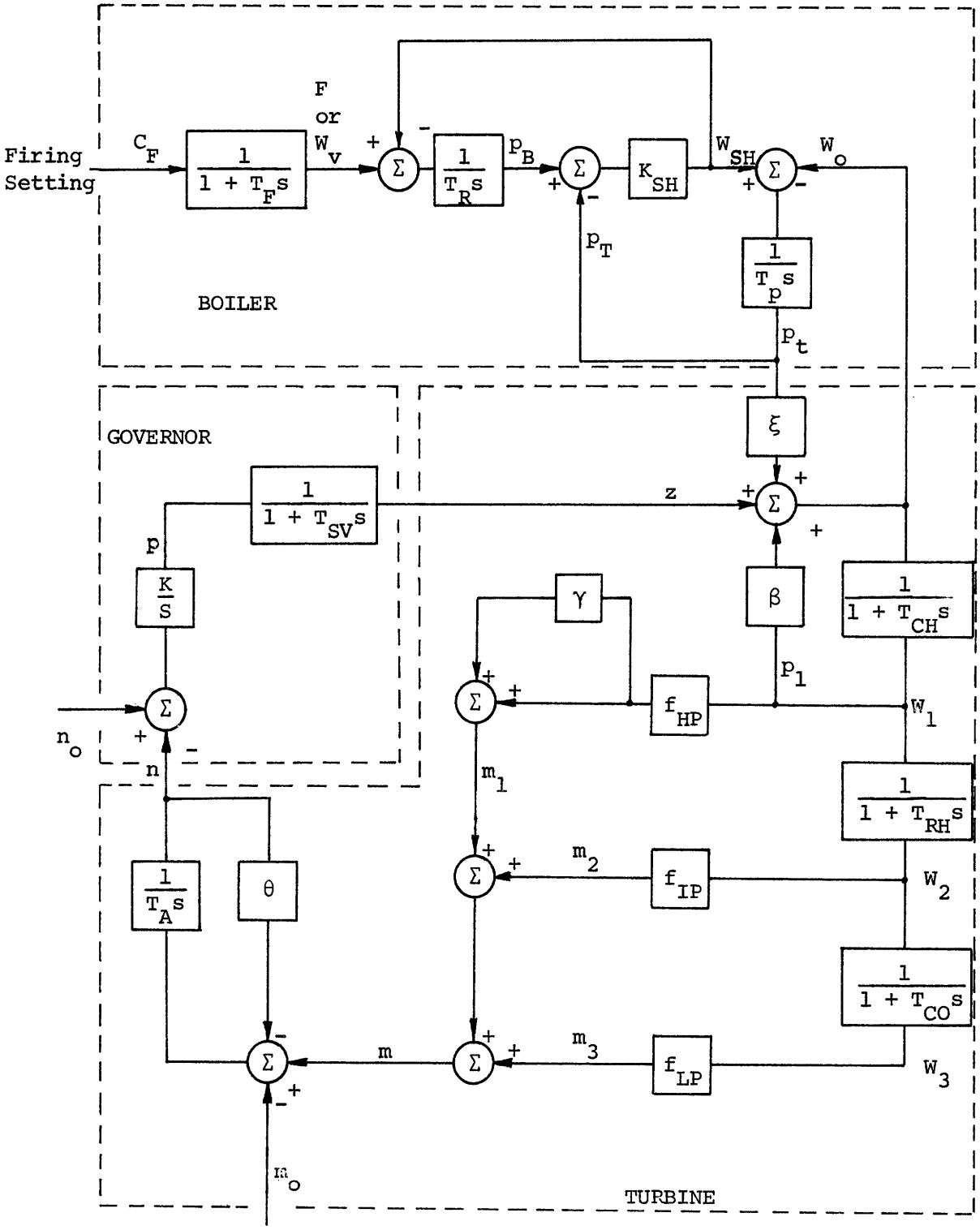

Fig. 13 Plant Model

III. APPLICATION OF CONTROLLERS

III.1 General

The complete plant model (8th order) is obtained by coupling together the boiler and the turbine models. It can be seen that the two models present very different response characteristics. While the boiler's large accumulation capacity makes its response very slow, the relatively small storage capacity of the steam turbine, even including the reheater, makes its response very fast.

The turbine load (output torque) is controlled by the speed governor which constitutes a "self-regulating" loop. A typical hydraulic governor is used in this system based on the available literature (see Chapter II.2.3), and a value within the usual range was given to the governor gain [speed droop = inverse of gain = 6%] which proved to be suitable for our purposes.

The change in load demand represented by the value of the input m_o (see Fig. 12) results in a torque unbalance which will cause rotor acceleration (or deceleration). Thus the valve stroke z is affected and changes both the main steam flow to the turbine and also the throttle pressure. The change in valve stroke is in the right direction to bring the turbine output closer to the load demand.

It can be seen that changes in valve stroke result in pressure disturbances to the boiler loop. The boiler controller then reacts to bring the pressure back to its original (set point) value. We attempt to find a suitable controller to perform this task with minimum oscillation and within a short period of time.

The reason why the pressure control of the boiler is treated in detail and no attention is given to the other loops can be justified in a number of ways. Basically, the fuel flow control to guarantee a proper burning rate is the most important factor in a boiler control. Its associated air flow rate is more easily controlled as it is approximately a zero-order system; i.e., the ratio of the stored mass in the gas circuit to its throughput is relatively small [1]. The same reasoning can be applied to the water level control which is one of the most important under the point of view of boiler safety. It is assumed, then, that a satisfactory control of those variables can be accomplished without difficulty. Another important variable to be controlled is the main steam temperature under the point of view of both safety and efficiency. In this case it cannot be considered a zero-order system but, instead, a very slow responding loop. Nevertheless, it is again the case of an internal loop in the sense that it does not affect the fuel input rate but rather makes changes in the energy distribution internally in the system.

Of course, the design of those "secondary loops" is not an easy task due to the cross-coupling between them. For example, a change in the air flow sensibly affects the energy distribution through the gas path and consequently affects the steam temperature and also the drum pressure. Changes in pressure affects the water level in the drum and also the steam flow and thus affects the feedwater flow into the boiler.

It is clear, however, that a certain load output determines a unique value for the fuel feed rate if we neglect small variation in

boiler efficiency, and the main problem which remains is to find a suitable control system.

III.2 Classical Control

Classical control systems are extensively used in existing power stations [1,6,8]. The combustion control is usually of the PID type (Proportional-plus-Integral-plus-Derivative), and the main problem is to correctly choose the values of the gain and of the integral and derivative time constants to achieve the "best" response. A certain degree of engineering judgement and experience are necessary to establish what the best response looks like, and usually it is translated to a group of specification statements: a certain percentage overshoot, a certain settling time, and so on. During the design period it is possible to determine the range of parameter values to meet the specifications, but the final values are always obtained by properly "tunning" the control system by a trial-and-error procedure.

We assume that a proper tunning has been made, and as a result the values of the control parameters have been determined. Actually, we use the PID control for rapid firing unit as given in the reference [6] but with a somewhat different arrangement of the derivative action. Later we will try to improve the system response by a change in parameters. In Fig. 14 we present the complete power plant model with the controller.

Step responses have been obtained for changes in load demand and also for changes in the control valves' position, for both 90% and 60% load level. The eigenvalues were computed for future comparison with optimal control approach.

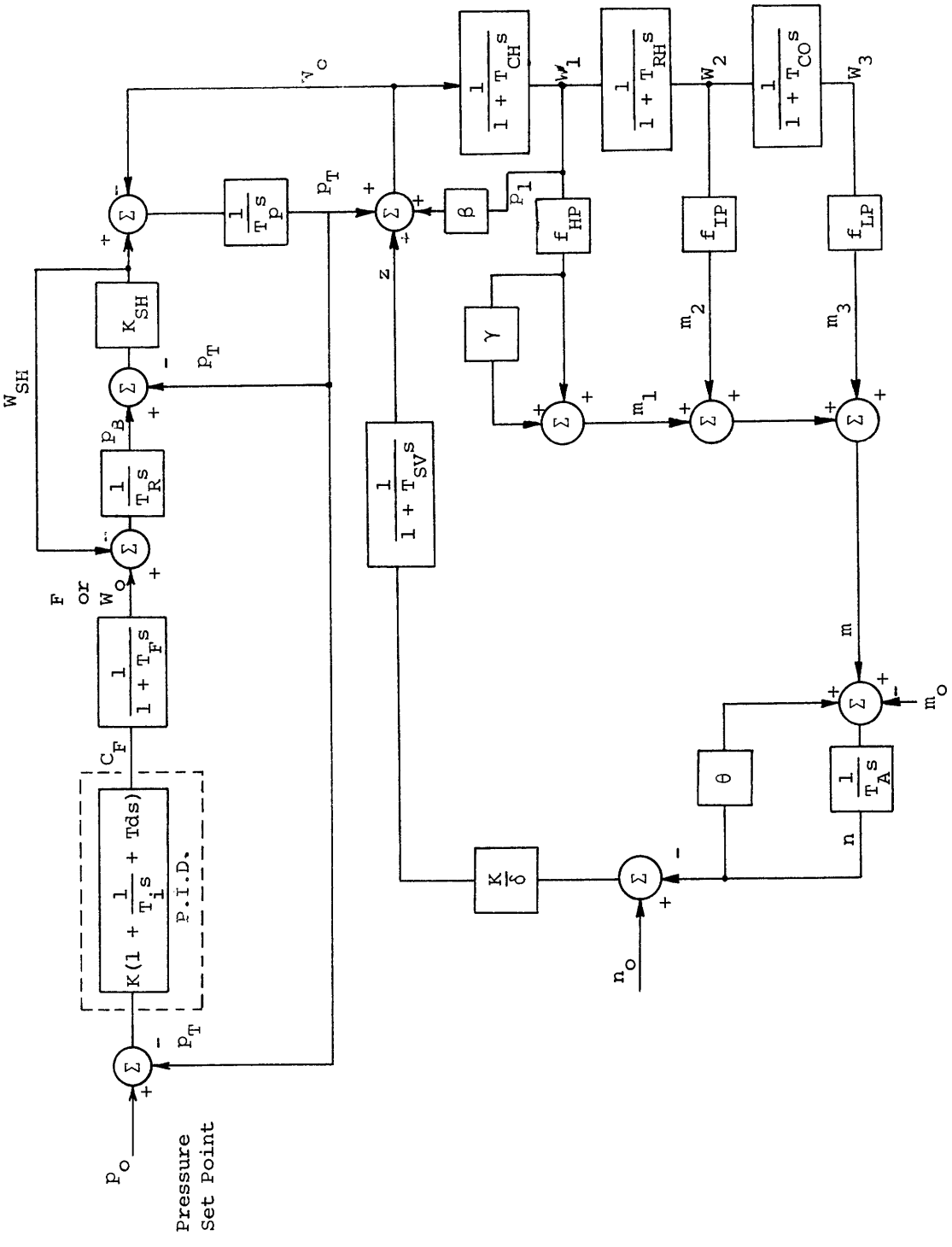

Fig. 14 Plant with PID Controller

The system is 9th order. The differential equations are presented as follows:

$$\dot{F} = \frac{1}{T_F}(C_F - F) \qquad (38) \text{ - Firing Rate}$$

$$\dot{p}_B = \frac{1}{T_R}[F - K_{SH}(P_B - P_T)] \qquad (39) \text{ - Drum Pressure}$$

$$\dot{p}_T = \frac{1}{T_R}[K_{SH}\, p_B - (K_{SH} + \xi)\, p_T - z - \beta\, W_1] \qquad (40) \text{ - Throttle Pressure}$$

$$\dot{W}_1 = \frac{1}{T_{CH}}(W_o - W_1) \qquad (41) \text{ - 1st Stage Flow}$$

$$\dot{W}_2 = \frac{1}{T_{RH}}(W_1 - W_2) \qquad (42) \text{ - Reheater Flow}$$

$$\dot{W}_3 = \frac{1}{T_{CO}}(W_2 - W_3) \qquad (43) \text{ - Cross-over Flow}$$

$$\dot{n} = \frac{1}{T_A}(m - m_o - \theta\, n) \qquad (44) \text{ - Speed}$$

$$\dot{z} = \frac{1}{T_{SV}}[\frac{K}{\delta}(n_o - n) - z] \qquad (45) \text{ - Valve Stroke}$$

$$\dot{C}_F = K(1 + Ti\frac{d}{dt} + TiTd\frac{d^2}{dt^2})(p_o - p_T) \qquad (46) \text{ - Control Output}$$

The last equation has to be developed in terms of the other state variables. This is accomplished in Appendix III to give:

$$\dot{C}_F = -CF\cdot F + CPB\cdot p_B + CPT\cdot p_T - CW1\cdot W_1 + CN\phi\cdot(n_o - n) - Cz\cdot z + CP\phi\cdot p_o \qquad (47)$$

where

$$CF = \frac{T_i Td}{T_p} \cdot \frac{K_{SH}}{T_R} \quad \frac{K}{T_i} \tag{48}$$

$$CPB = \frac{\chi K_{SH}}{T_p} + \frac{T_i Td}{T_p} \quad \frac{K_{SH}^2}{T_R} \quad \frac{K}{T_i} \; ; \quad \chi = \frac{T_i Td}{T_p} \; (\quad + K_{SH}) - T_i \tag{49}$$

$$CPT = -\frac{\chi}{T_p} \; (\xi + K_{SH}) - 1 + \frac{T_i Td}{T_p} \; (\frac{\beta\xi}{T_{CH}} - \frac{K_{SH}^2}{T_R}) \quad \frac{K}{T_i} \tag{50}$$

$$CW1 = \frac{\chi\beta}{T_p} \quad - \quad \frac{T_i Td}{T_p} \quad \frac{\beta(\beta - 1)}{T_{CH}} \quad \frac{K}{T_i} \tag{51}$$

$$CN\phi = \frac{T_i Td}{T_p T_{SV}} \; (\frac{K}{\delta}) \quad \frac{K}{T_i} \tag{52}$$

$$Cz = \frac{\chi}{T_p} + \frac{T_i Td}{T_p} \; (\frac{1}{T_{SV}} - \frac{\beta}{T_{CH}}) \quad \frac{K}{T_i} \tag{53}$$

$$CP\phi = \frac{K}{T_k} \tag{54}$$

A simpler and perhaps more suitable form also used in the computations was derived in Appendix III by considering the controller as composed by three parallel-connected elements. The firing setting takes the form:

$$C_F = - Kp_T + C_{F2} - KTd \; \dot{p}_T$$

where C_{F2} is obtained from

$$\dot{C}_{F2} = - \frac{K}{T_i} \; p_T \; .$$

In this last form it is easier to visualize the additional state introduced by the integral controller.

To solve those equations and to obtain a plot of the time response of state variables, we utilized the DYSYS program (DYnamic SYstems Simulator) available at the Joint Computer Facility of the Mechanical and Civil Engineering Departments. The subroutine EQSIM used to set up the differential equations can be adapted to use any other available program without much difficulty. To compute the eigenvalues we used either ACCESS or the EISPAC subroutine. A rescaling was found to be necessary to get correct values of the eigenvalues when using PID control due to the large difference in the order of magnitude of the coefficients in the differential equations. By such reason, some of the plots of results with PID are in a rescaled frame. The original scaling, as mentioned previously, is in per-unit values of steady-state conditions.

The results are presented in Chapter III-4 where a comparison is made with the optimal control approach.

III.3 Modern Control Approach

The differential equations of the open-loop plant model can be put into a standard form as follows:

$$\dot{\underline{x}} = \underline{A}\,\underline{x} + \underline{B}\,\underline{u} \qquad (55)$$

where $\underline{x}$ is the vector of state variables; (8 x 1)

$\underline{u}$ is the vector of inputs;

$\underline{A}$ is the system matrix (8 x 8) composed by the coefficients of the differential equations; and

$\underline{B}$ is the control matrix composed by the coefficients of established inputs.

Although we have three possible inputs (firing setting, speed, and load references), we are directly interested in the control of the firing rate. Thus we consider as input the firing setting and treat the other two as possible disturbances into the system. With such arrangement, we deal with a single input system, and $\underline{B}$ becomes a 8 x 1 vector.

The modern control approach consists in finding the optimal control law u^o in order to minimize a quadratic objective function of the form (for further details, see ref. [14]).

$$V = \frac{1}{2} \int_o^\infty [\underline{x}^T \underline{Q} \underline{x} + u^T R u] \, dt \tag{56}$$

where $\underline{Q}$ is symmetric and at least positive semi-definite and

$R > 0$ (in the general case, $\underline{R}$ must be symmetric and positive definite).

This structure corresponds to the so-called linear Quadratic Regulator (LQR) problem.

The optimal control law is given by

$$\underline{u} = \underline{G} \underline{x} \quad , \text{ where} \tag{57}$$

$$\underline{G} = - R^{-1} \underline{B}^T \underline{S} \quad \text{controller gain matrix} \tag{58}$$

and $\underline{S}$ is obtained solving the Reduced Matrix-Ricatti equation, of the form:

$$\underline{O} = \underline{SA} - \underline{A}^T \underline{S} + \underline{SB} R^{-1} \underline{B}^T \underline{S} - \underline{Q} \quad . \tag{59}$$

The numerical solution of the reduced Matrix-Ricatti equation is readily obtained through the ACCESS program functions available in the Joint Computer Facility.

The key point in the use of the optimal control approach is the proper selection of $\underline{Q}$ and $\underline{R}$ matrices. Each $\underline{Q}$ and $\underline{R}$ combination

constitutes a different optimal policy. We adopted the usual procedure of choosing the diagonal elements of the $\underline{Q}$ matrix taking the inverse of the square of maximum allowable deviations of each corresponding state variable:

$$\underline{Q} \equiv \begin{bmatrix} \frac{1}{x_{1m}^2} & 0 & 0 & \cdots & 0 \\ 0 & \frac{1}{x_{2m}^2} & 0 & \cdots & 0 \\ 0 & 0 & \frac{1}{x_{3m}^2} & \cdots & 0 \\ \hline 0 & 0 & 0 & \cdots & \frac{1}{x_{nm}^2} \end{bmatrix} \tag{60}$$

It is sufficient, in our case, to weight the variables x_1 and x_3 only, corresponding to the firing intensity and throttle pressure, respectively. The limitation of the firing rate is necessary because of the implied capital costs of the fuel supply system, and the limitation of the throttle pressure is necessary to prevent excessive excursions which would adversely affect the turbine performance. The other variables, as the drum pressure and steam flow from the boiler, depend directly on the firing intensity and throttle pressure, and so they are automatically limited. The variables related to the turbine-governor system are subjected to a separate control (the turbine governor) and do not have to be weighted.

The $\underline{R}$ matrix is obtained in a similar way, and in our particular case, it takes the form:

$$R \equiv \left[\frac{1}{u_m^2} \right] \tag{61}$$

where u_m is the maximum allowable deviation in the input variable.

The details of the $\underline{Q}$ and R matrices are presented in Appendix IV.

One problem with the optimal control approach by the use of Matrix-Ricatti equation alone is that there is no integral action in the resulting controller. For systems with a free integrator in the forward path, it does not constitute a problem because zero steady state error can be achieved by making the gain corresponding to the variable under consideration equal to unity. As this is not the case of our system, it was necessary as a next step to use an "optimal integral control" approach which combines the Matrix-Ricatti and an integral controller [14]. Such approach can be synthesized as follows:

$$\dot{\underline{x}} = \underline{A}\,\underline{x} + \underline{B}\,\underline{u} \qquad (62) \text{ - System Equation;}$$

$$\dot{\underline{u}} = \underline{V} \qquad (63) \text{ - Integral Controller Output;}$$

$$y = \underline{H}\,\underline{x} + \underline{D}\,\underline{u} \qquad (64) \text{ - The Output, where } \underline{D} = 0 \text{ in our case;}$$

We take:

$$\underline{x} = \left[\begin{array}{c} \underline{x} \\ \hline \underline{u} \end{array} \right] \qquad (65) \quad \text{Augmented State Vector;}$$

$$\dot{\underline{\overline{x}}} = \underline{\overline{A}}\,\underline{\overline{x}} + \underline{\overline{B}}\,\underline{v} \qquad (66) \quad \text{Equivalent System Equation;}$$

$$\underline{y} = \underline{\overline{H}}\,\underline{\overline{x}} \qquad (67) \quad \text{Equivalent Output;}$$

where

$$\bar{A} = \left[\begin{array}{c|c} A & B \\ \hline 0 & 0 \end{array}\right] \quad ; \quad \bar{B} \equiv \left[\begin{array}{c} 0 \\ \hline 1 \end{array}\right] \quad ; \quad \bar{H} \equiv \left[\begin{array}{c:c} H & D \end{array}\right] \tag{68}$$

and take a new objective function

$$J = \frac{1}{2} \int_0^\infty [y^T Q y + v^T R v] \, dt \quad . \tag{69}$$

Now, v is obtained by

$$v = G \bar{x} \equiv G_1 x + G_2 u \tag{70}$$

where $$G = - R^{-1} \bar{B}^T \bar{S} \tag{71}$$

and $\bar{S}$ is obtained by solving the reduced Matrix-Ricatti equation for the modified system:

$$0 = - \bar{S} \bar{A} - \bar{A}^T \bar{S} + \bar{S} \bar{B} R^{-1} \bar{B}^T \bar{S} - Q \tag{72}$$

The resulting system is shown in Fig. 15.

A more convenient equivalent form is available, where the integral control is shown to be a direct function of the error $y - y_o$. Such structure is shown in Fig. 16 where

$$[L \,|\, C_y] \equiv [G_1 \,|\, G_2] \left[\begin{array}{c|c} A & B \\ \hline H & D \end{array}\right]^{-1} \tag{73}$$

We used the last form of equation (73) in our system. The Q matrix was obtained exactly as before but augmented with one additional row and column. (See Appendix IV) Simulation results are presented in Chapter III-4. In Fig. 17 the block diagram of the system is shown with the optimal integral controller. The controller gains are presented in Table 7 of Appendix IV.

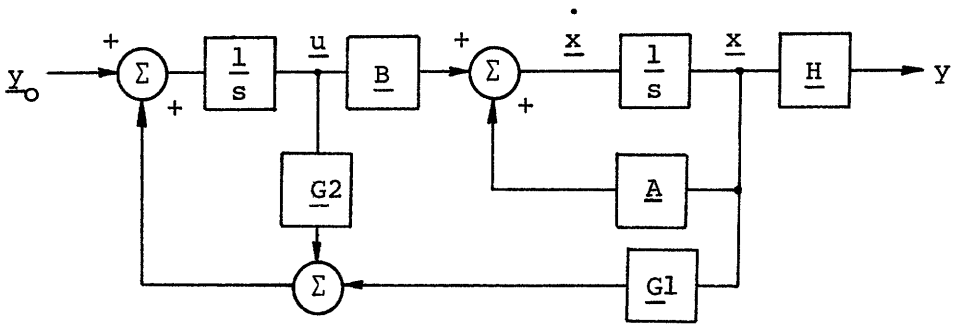

Fig. 15 Optimal Integral Controller

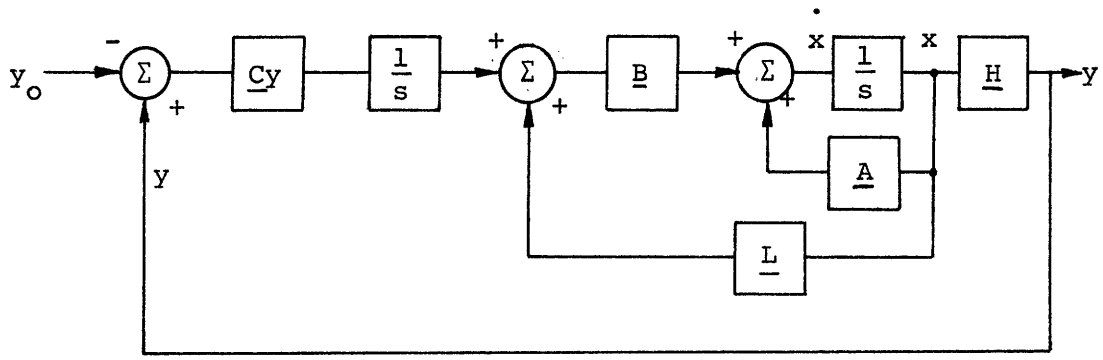

Fig. 16 Equivalent Optimal Integral Controller

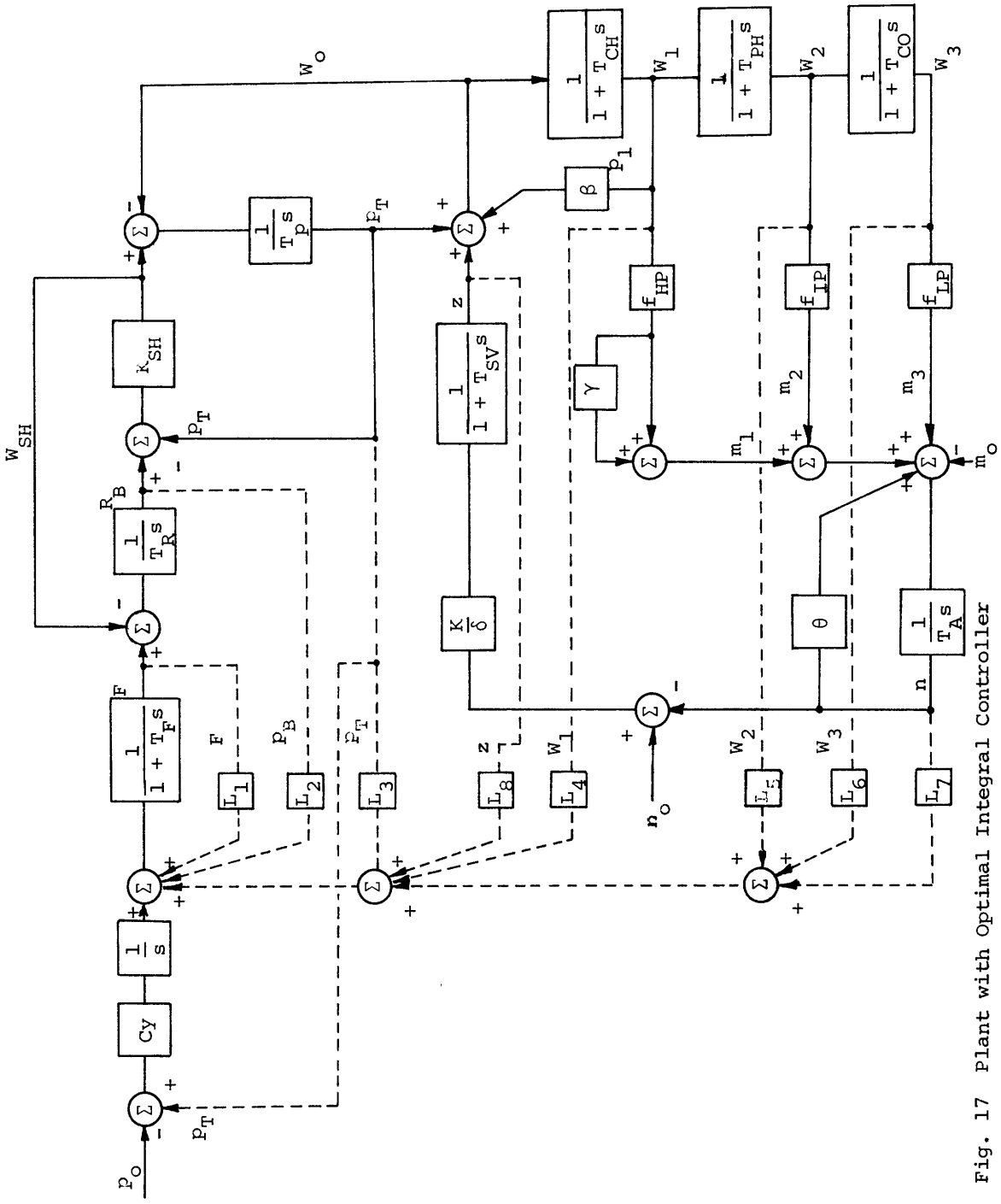

Fig. 17 Plant with Optimal Integral Controller

III.4 Comparison of Results

III.4.1 General

The results of the simulation are presented in Figs. 18 through 32, for different load levels.

At 90% load level the step increase in load demand was limited to 5% due to the limited capacity of the fuel supply system. At 60% load level a step increase of 10% was assumed.

During the first 15 seconds, there are transient oscillations of pressure, valve stroke, turbine load, and steam flow, as shown in detail in the enlarged time scale of Fig. 19. These transients are caused by the normal speed-governor action to bring the turbine output torque to the new demand level in order to keep the turbine shaft speed at its nominal value. It is interesting to note that the turbine response is practically the same for any value of PID parameters and even with the Optimal Integral Controller. This similarity is also evidenced by comparing the "fast" eigenvalues in Tables 4 and 5. On the other hand, the boiler response is considerably affected by a change of controller parameters.

In comparing the results the settling time is used. It is determined as the time required to bring the final value of the variable within $\pm$ 5% of the new steady-state value. In the case of pressure whose steady-state value is zero, another criterion was used. It was assumed that a commercially available instrument with an enlarged (+ 50 psi; - 100 psi) scale about the nominal pressure is used in the plant to measure the pressure with an accuracy of about 5% of the full scale, and the settling time was assumed to be the time necessary to

PID Controller; T_i = 45; Td = 20						Optimal Controller R = [4]	
K = 4.5		K - 6.0		K = 20.0			
-14.08	--	-14.06	--	-13.85	--	-14.15	--
- 4.61	--	- 4.61	--	- 4.61	--	- 4.61	--
- 2.07	+j .419	- 2.07	+j .419	- 2.07	+j .420	- 2.07	+j .419
- 2.07	-j .419	- 2.07	-j .419	- 2.07	-j .420	- 2.07	-j .419
- .365	+j .782	- .364	+j .782	- .356	+j .783	- .367	+j .789
- .365	-j .782	- .364	-j .782	- .356	-j .783	- .367	-j .789
- .151	--	- .171	--	- .380	--	- .318	+j .310
- .00992	+j .0204	- .0118	+j .0225	- .0197	+j .0234	- .318	-j .310
- .00992	-j .0204	- .0118	-j .0225	- .0197	-j .0234	- .0258	--

Table 4 System Eigenvalues - 90% Load Level

PID Controller K = 4.5; T_i = 45; Td = 20		Optimal Controller R = [4]	
-20.20	--	-20.24	--
- 4.679	--	- 4.679	--
- 2.060	--	- 2.058	--
- 1.854	--	- 1.858	--
- 0.455	+j 0.844	- 0.454	+j 0.847
- 0.455	-j 0.844	- 0.454	-j 0.847
- 0.125	--	- 0.396	--
- 0.00614	+j 0.0163	- 0.240	--
- 0.00614	-j 0.0163	- 0.0284	--

Table 5 System Eigenvalues - 60% Load Level

bring the pressure within $\pm$ 1.4 x 10^{-3} in per unit value, based on the instrument's accuracy

The extreme values for the throttle pressure and firing rate as well as the settling time are presented in Table 6.

An upper limit in the control signal is also considered, although it depends on the controller design. It is assumed that an increase of about 100% over the normal operating level is admissible, but it was not considered a rigid limit, as it is not a physical limitation of the plant itself.

III.4.2 Results with PID Controller

The results for 5% step increase in load demand and with initial PID settings : K = 4.5, T_i = 45, and Td = 20, are presented in Fig. 18. The following points are noted:

- The valve stroke z closely follows the pressure deviations but in the opposite direction to keep the load as steady as possible. This action is the result of the effective governor control. Small oscillations in the torque output and throttle flow are not noticeable in the graph after about 15 seconds.

- The per-unit increase in throttle flow is less than the increase in torque. In our model this action is due to the γ factor (see Eq. 35). The first stage pressure increases when the load increases, and as a consequence there is an increase in the H.P. turbine enthalpy drop which contributes to reduce the additional flow necessary to maintain the new load level.

- The throttle pressure decreases steeply at first and then increases again following the valve stroke excursions (see Fig. 19). The increase

Load Level (%)	Controller	Extreme (Per-Unit Values)					Settling Time (Seconds)	
		P_T		F				
		Min.	Max.	Min.	Max.	% Overshoot	P_T	F
90	PID; K = 4.5, T_i = 45; Td = 20	-.0062	.0013	0.	.055	25	120	262
	Optimal; R = [4]	-.0059	0.	0.	.057	30	42	70
	PID; K = 4.5, Td = 20, T_i = 10	-.0055	.0034	0.	.068	55	295	480
	PID; K = 4.5, Td = 20, T_i = 20	-.0054	.0026	0.	.061	39	155	280
	PID; K = 4.5, T_i = 45, Td = 30	-.0055	.0013	0.	.065	48	130	292
	PID; K = 4.5, T_i = 45, Td = 40	-.0056	.0014	0.	.083	89	150	316
	PID; T_i = 45, Td = 20, K = 3	-.0084	.0024	0.	.058	32	270	335
	PID; T_i = 45, Td = 20, K = 6	-.0054	.0008	0.	.060	36	103	154
	PID; T_i = 45, Td = 20, K = 20	-.0045	.0003	-.0017	.110	150	38	82
	PID; T_i = 45, Td = 20, K = 30	-.0044	.0002	-.0022	.110	150	28	64
	PID; K = 20, T_i = 45, Td = 40	-.0043	.0006	-.0450	.110	150	50	100
	PID; K = 20, T_i = 45, Td = 60	-.0042	.0009	-.0685	.110	150	60	125
60	PID; K = 4.5, T_i = 45, Td = 20	-.0113	.0034	0.	.123	33	340	390
	Optimal; R = [4]	-.0045	0.	0.	.116	25	55	85

Table 6 Comparison of Results

in firing intensity at this stage is not sufficient to bring the pressure back to its normal level, and a further decrease takes place. The minimum pressure is reached at about 40 seconds and normal level at about 120 seconds.

- The overshoot in firing intensity is reasonable (25%). We will see that attempts to reduce the settling time by changing the PID parameters adversely affects the overshoot in firing.

- The calculated oscillation period of the throttle pressure, based on the imaginary part of the corresponding eigenvalue, is about 308 seconds. The settling time is therefore within half cycle of oscillation which means a good damping characteristic.

Results with changes in PID parameters are shown in Figs. 20 to 24.

Decreasing the integral time alone causes the oscillation period to decrease and the settling time to increase. Also, the overshoot in firing rate is increased as the result of heavier oscillations (Fig. 20).

Increasing the derivative time alone also resulted in an increase of settling time and of overshoot in firing intensity. In this case, however, such overshoot occurs during the turbine transients unlike in the previous cases, where the overshoot occurred during the low boiler transients. This fact is hardly seen in the plots due to the difference in the oscillation frequency of the boiler and turbine. However, in Fig. 19 we can see the "initial overshoot" in firing rate. Actually with increased derivative time, the upsurge during the boiler transient is less than with the initial settings.

Increasing the controller gain decreases the settling time as can be seen in Figs. 22 to 24 and Table 6. With K = 20 the settling time is

of the same order as with Optimal Integral Controller. On the other hand, the firing intensity reaches the upper limitation imposed by the fuel system, corresponding to 150% overshoot. Also, the controller output (not plotted) reaches a maximum of the order of 1.3 which represents too high a level even for a control signal.

Responses were also obtained at 60% load level for 10% step increase in load demand. The results are shown in Fig. 25 and 26. Except for the slower response due to the increase in the relative accumulation capacity of the boiler, the same conclusions may be adopted.

Also, a step response to a 5% negative step change in valve stroke was obtained at 90% load level. This is somewhat an artificial condition as the valve stroke is a function of the speed error, and in this case it was set independently at a certain value. The load demand was made to exactly follow the output torque, i.e., keeping the speed constant at its normal level. From the response in Fig. 27, it can be seen that the load stabilization time is of the same order as the pressure settling time.

The steep pressure increase during the first 3 or 4 seconds is due to the low accumulation capacity of the steam piping (T_p = 1.5 sec). Its inclusion in the boiler model was to simulate such behaviour, typical in steam power plants. Also, the steam flow and load responses are typical patterns for steam plants.

III.4.3 Results with Optimal Integral Controller

Responses were obtained with Optimal Integral Controller at 90% load and 5% step increase in load demand, for values of R (weight on

input variable C_F) equal to [0.25], [4.0], and [25.0], corresponding to maximum allowable deviations of 20., 0.5, and 0.2 per-unit, respectively. In all cases the Q matrix (weight on state variables) was the same as developed in Appendix IV.

With R = [0.25] a good result was obtained (Fig. 28). The response was very smooth with 32% overshoot in firing rate and no oscillations. The settling time was only 145 seconds for firing rate and 85 seconds for pressure.

With R = [4.0] a better response was obtained (Fig. 29). The overshoot in firing intensity was 30%, and the settling time for pressure only 42 seconds. It can be noted in this case that the maximum downsurge in pressure is due to the maximum control valve opening. The firing system responds fast enough to prevent a further pressure decrease. The integral controller output was 1.10 thus indicating that a further improvement could not be made. In fact, with R = [25.] the output signal level reached 2.40, too high a level.

The notable aspect of the optimal integral controller, with R = [4.0], is the fast and smooth response of the firing intensity which is brought up to the new value within the first 10 seconds after the disturbance occurs.

The system eigenvalues with optimal controller still show that the turbine-side transients are the same order as with PID controller. On the boiler side, however, some changes occurred. The pressure lost its oscillatory behaviour, and also no oscillations are present in firing intensity.

Plant response was also obtained for 10% increase in load demand at 60% load level. The results are presented at Fig. 30 where it can be seen that the performance is still very good at the low load level.

Also, a step response to a change in control valve stroke was obtained at 90% load level and -5% step (Fig. 31). Comparing with PID controller at Fig. 27, it can be noted that the load stabilization period is cut in half, and pressure excursion is considerably minimized.

Due to the difficulty in getting good accuracy in flow measurement, we obtained a response supressing the measurement and feedback control of steam flows (Fig. 32). As a result the overshoot in firing rate increased to 68%, but its settling time decreased to about 60 seconds and also the pressure settling time decreased to 32 seconds. This was mainly due to the reheater steam flow effect, as its coefficient was predominant (see Table 7) compared with the first stage or the cross-over flows.

IV. CONCLUSIONS

From the study of power plant control characteristics, the following general conclusions can be deduced:

- The turbine response for sudden changes in load demand has been found to be practically independent of the type of boiler control. The fast governor action adjusts the control value opening to compensate for the temporary drop in the throttle pressure, allowing an additional amount of steam flow to the turbine. This fact validates the use of simplified turbine models without considering the dynamics of the boiler for stability studies of large interconnected systems when limited to short-period transients.

- The boiler and turbine responses can be adjusted independently by changing the boiler control parameters and the governor speed droop (δ), respectively. The eigenvalues' comparison shows only a weak dependance between the two responses.

- Optimal Integral Controller with full state feedback provides a better response than that of the PID controller considered. Under approximately the same settling time conditions, the firing intensity with the PID controller turns out to be very oscillatory with much greater overshoot than with optimal controller. These oscillations are a consequence of the valve stroke effects on throttle pressure. The optimal control system compensates the tendency for oscillation by "sensing" it through the other state variables and introducing an adequate correction.

If oscillations in the fuel system can be tolerated, then the PID controller can give results as good as with optimal controller by

conveniently adjusting the parameters. As the boiler is a good "filter" of disturbances due to its high accumulation capacity, the final throttle pressure is not affected by the relatively high frequency oscillations. However, higher efforts result in the fuel supply system, and consequently the design requirements and capital cost are affected.

- Supressing the feedback of steam flows increases the overshoot, but the good performance of the optimal controller is still maintained.

RECOMMENDATIONS FOR FUTURE WORK

As the next step to this work, we suggest that the attention be concentrated primarily on the boiler, and use only a simplified turbine in order to develop the optimal integral controller by:

1. Using iterative techniques [14] to find the most suitable form for the Q matrix.
2. Developing observers for inaccessible variables.

To compare the results with classical PID controller, we suggest inclusion of the first stage pressure feedback as an improvement to PID control.

Finally the validity of the results of this work could be verified also for turbine-follow and integrated control systems.

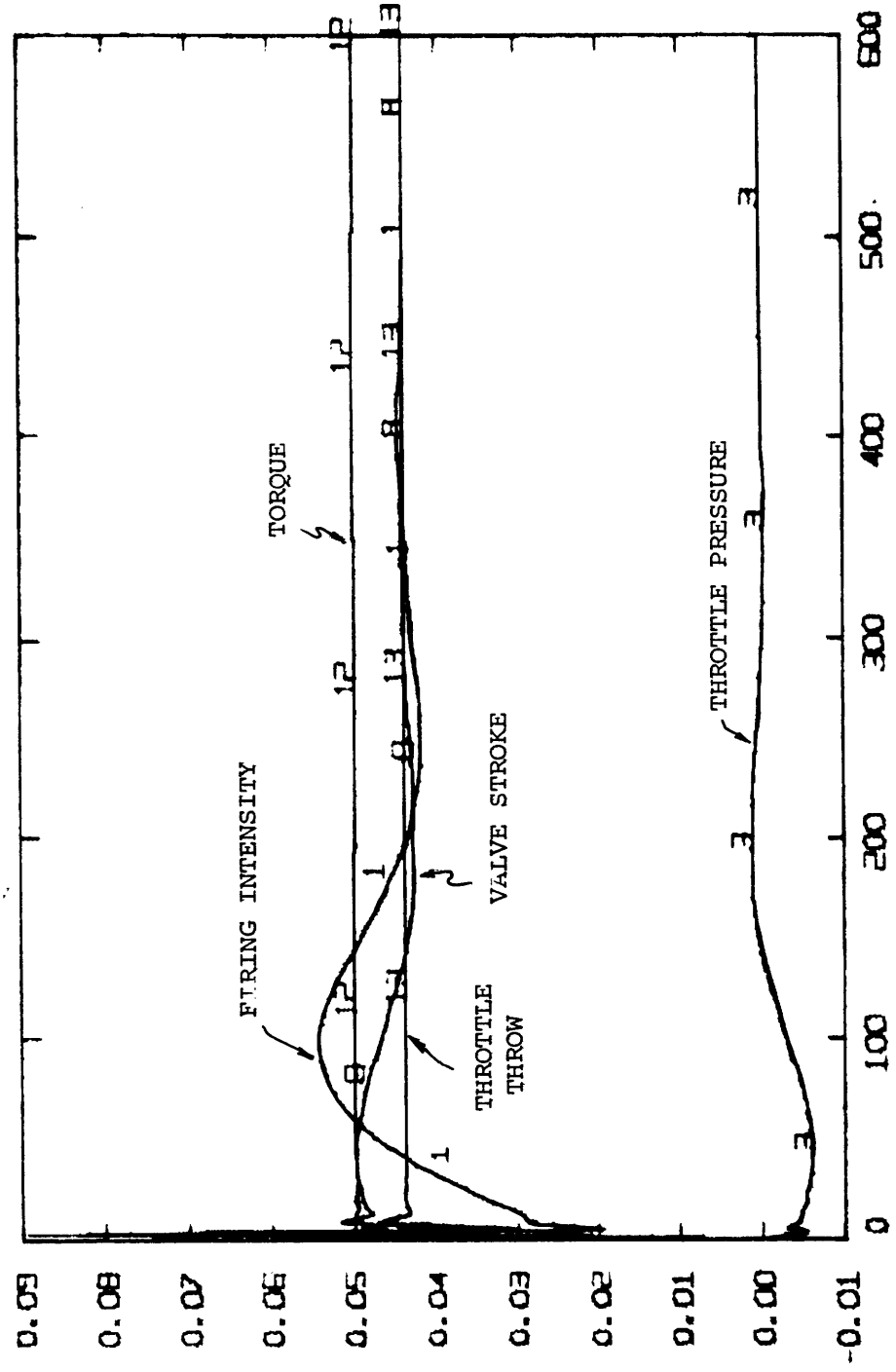

Fig. 18 Plant with PID Controller - 90% Load Level;
Response to 5% Step in Load Demand
$K = 4.5$; $T_i = 45$; $Td = 20$

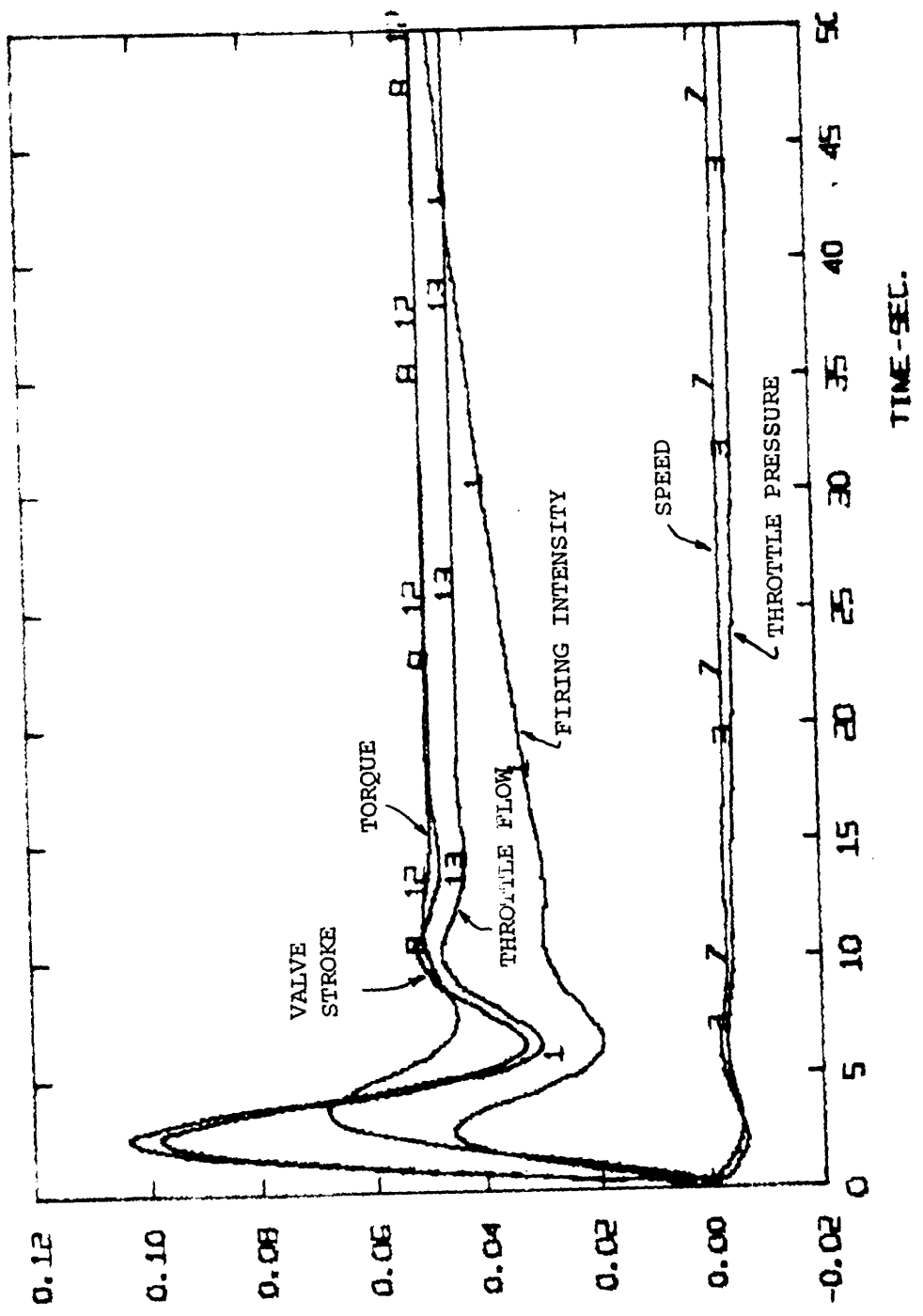

Fig. 19 Plant with PID Controller - 90% Load Level; 5% Step in Load Demand - Turbine Transients K = 4.5; T_i = 45; Td = 20

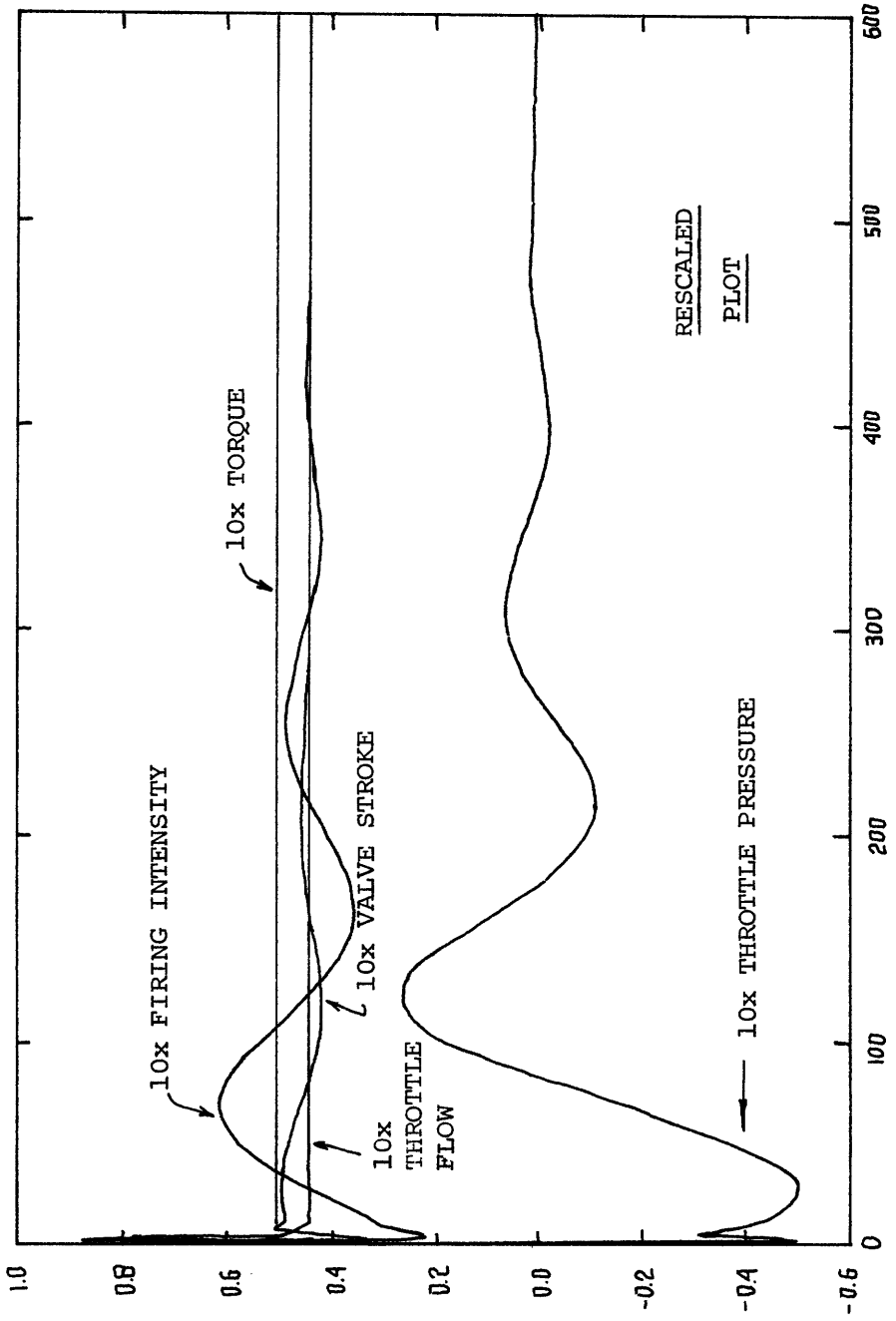

Fig. 20 Plant with PID Controller - 90% Load Level; 5% Step in Load Demand - Decreasing Integral Time
K = 4.5; T_i = 20; Td = 20

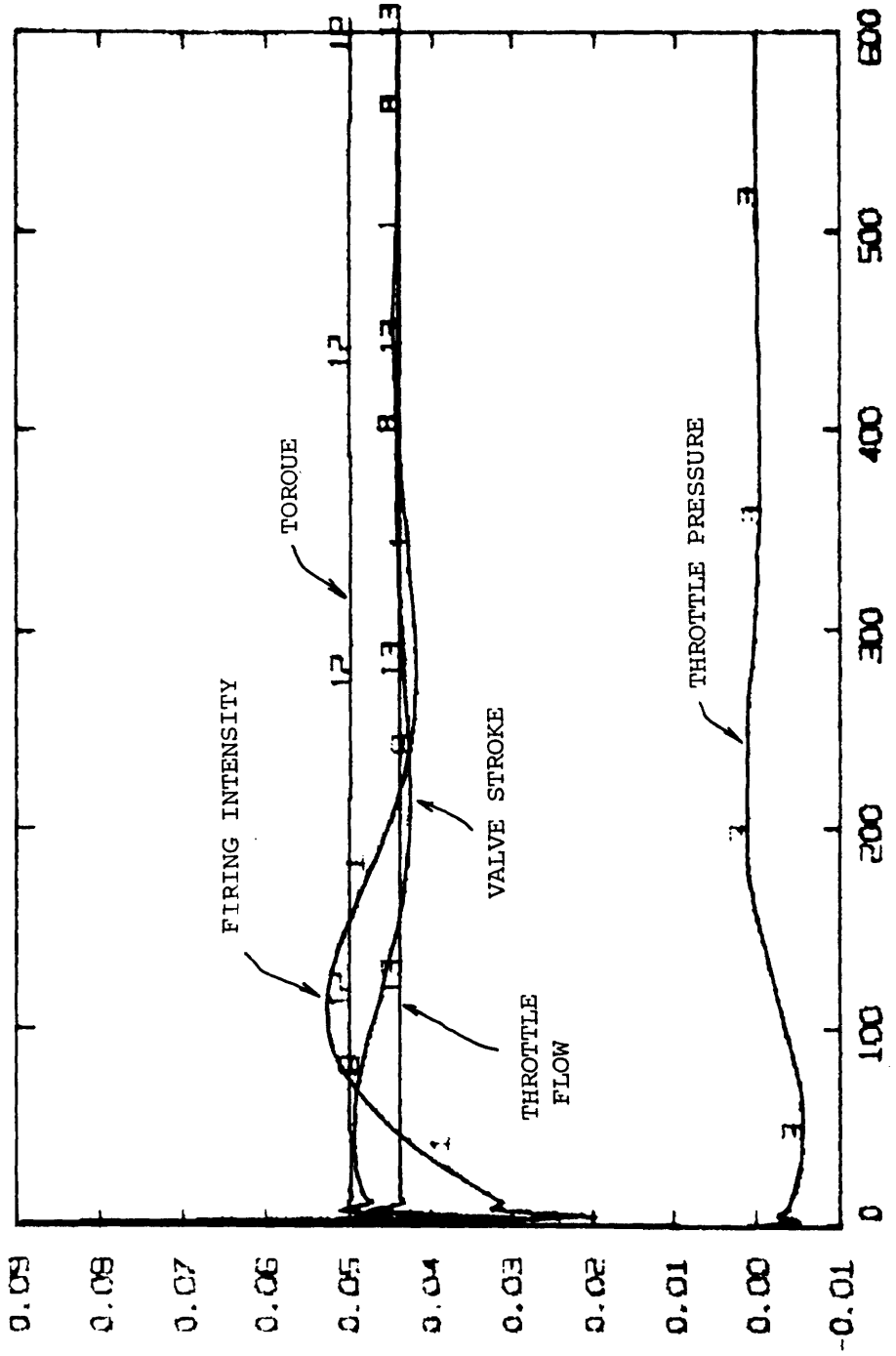

Fig. 21 Plant with PID Controller - 90% Load Level;
5% Step in Load Demand - Increasing Derivative Time
K = 4.5; T_i = 45; Td = 30

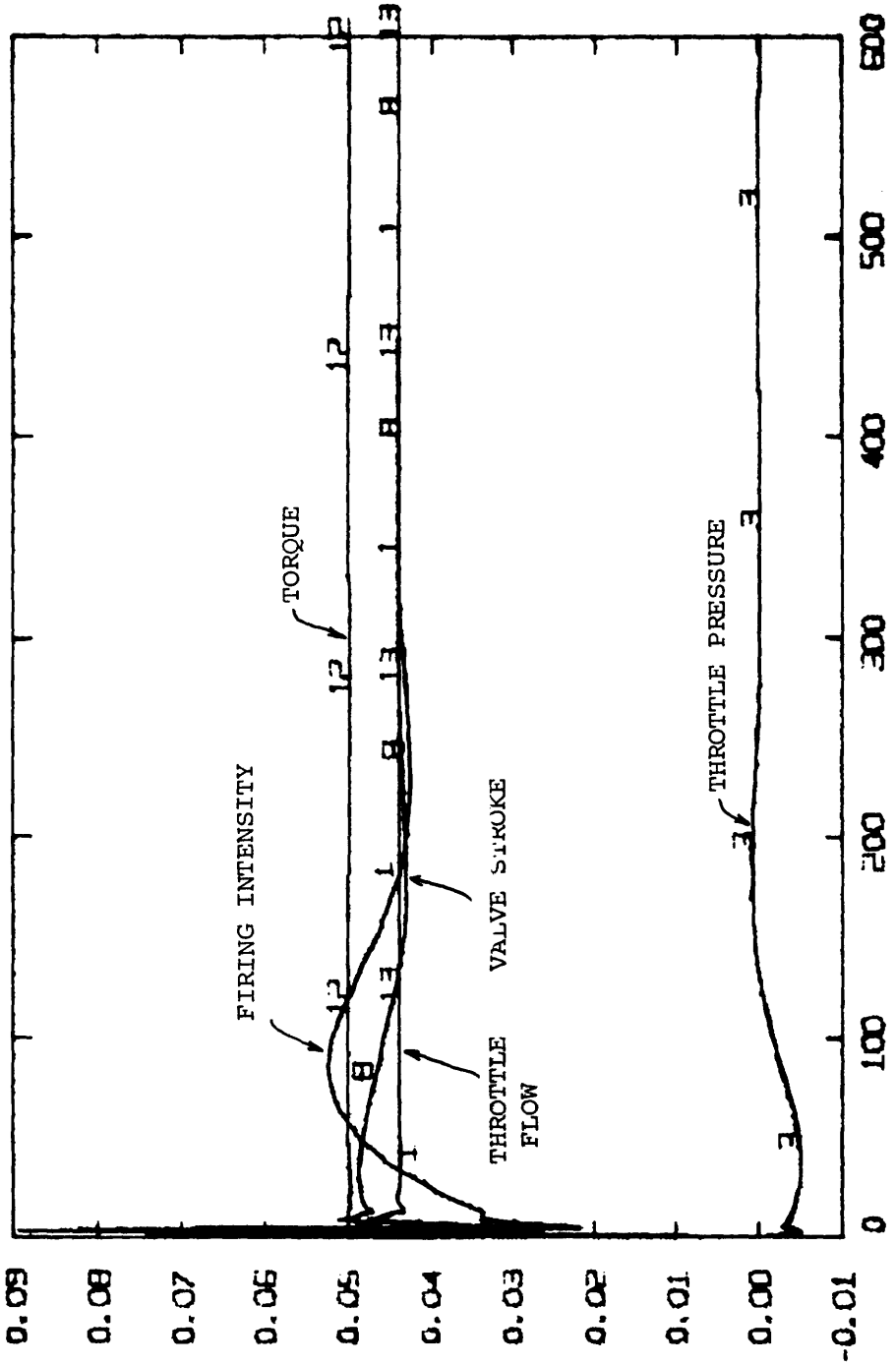

Fig. 22 Plant with PID Controller - 30% Load Level; 5% Step in Load Demand - Increasing Gain $K = 6.0$; $T_i = 45$; $Td = 20$

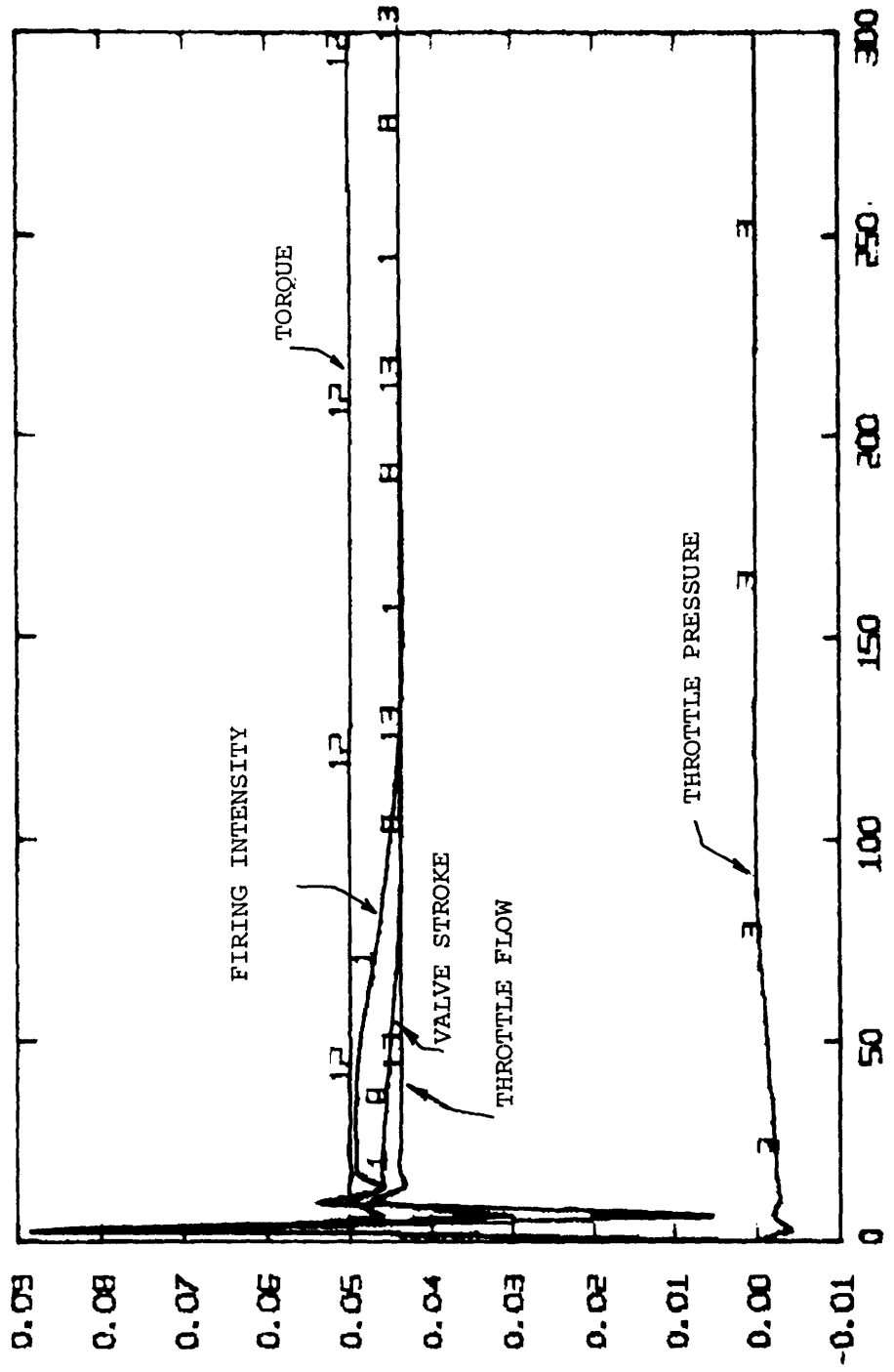

Fig. 23 Plant with PID Controller - 90% Load Level;
5% Step in Load Demand - Increasing Gain
$K = 20.0$; $T_i = 45$; $Td = 20$

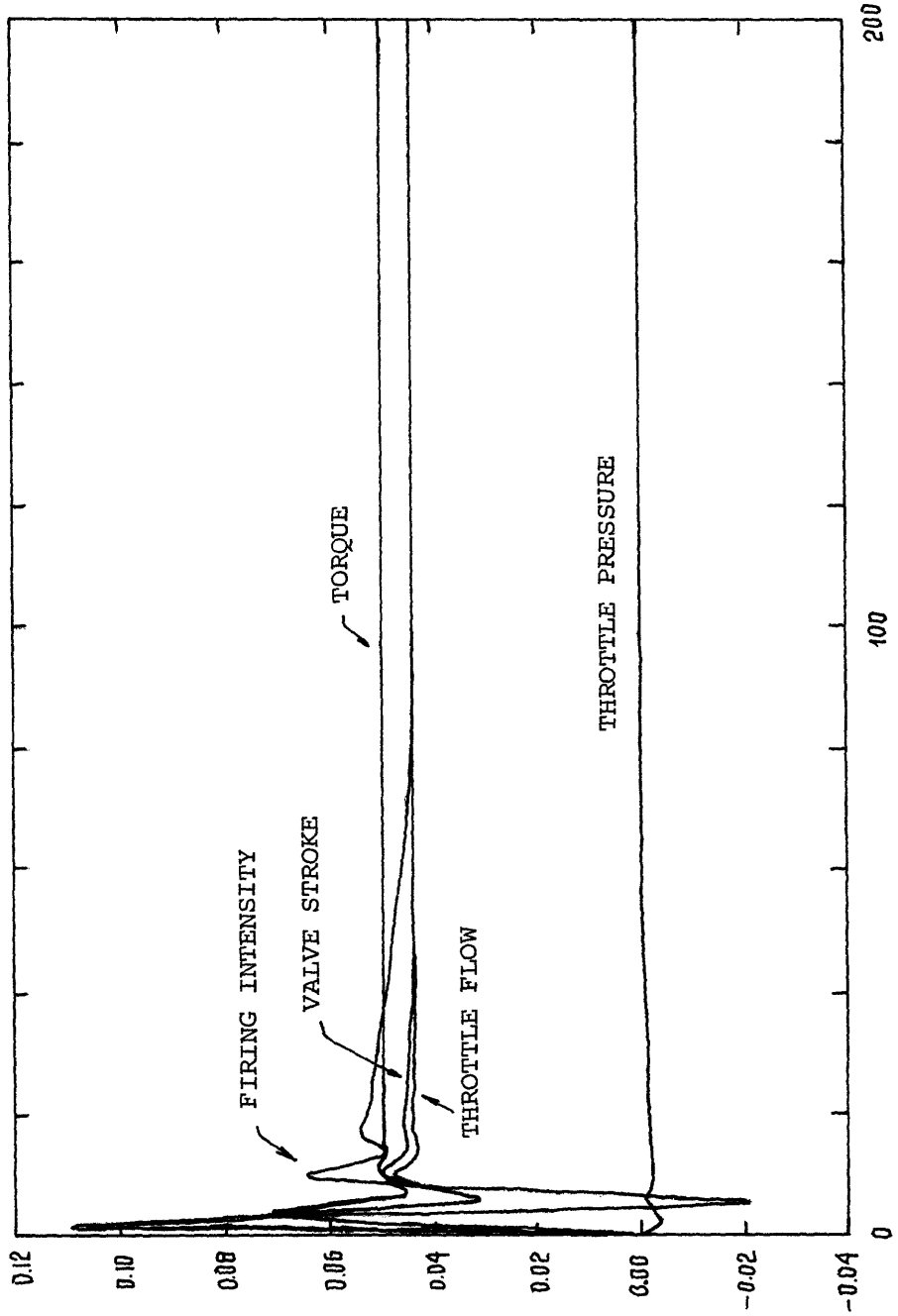

Fig. 24 Plant with PID Controller - 90% Load Level;
5% Step in Load Demand - Increasing Gain
K = 30.0; T_i = 45; Td = 20

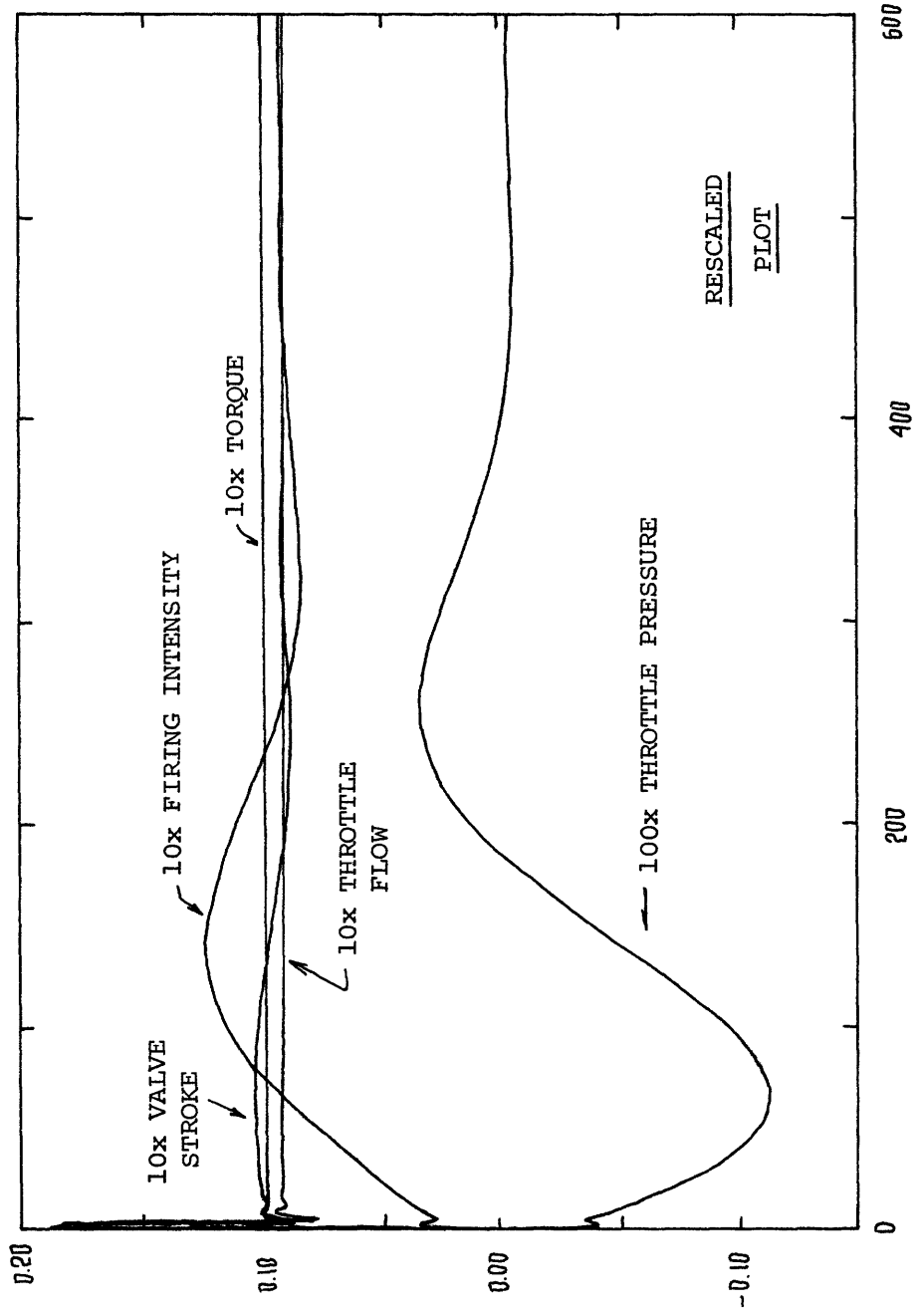

Fig. 25 Plant with PID Controller - 60% Load Level;
10% Step in Load Demand
K = 4.5; T_i = 45; Td = 20

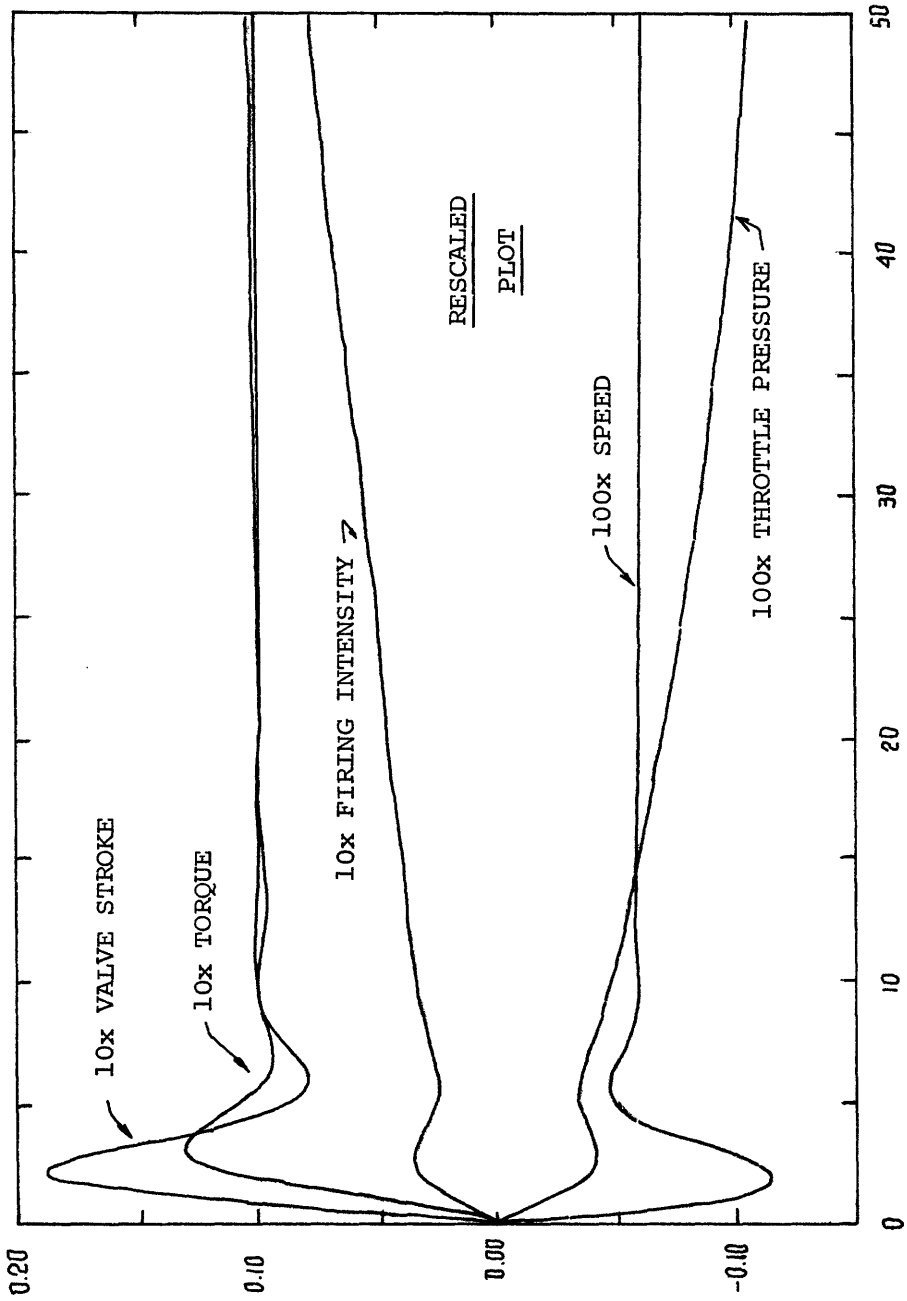

Fig. 26 Plant with PID Controller - 60% Load Level;
10% Step in Load Demand - Turbine Transients
K = 4.5; T_i = 45; Td = 20

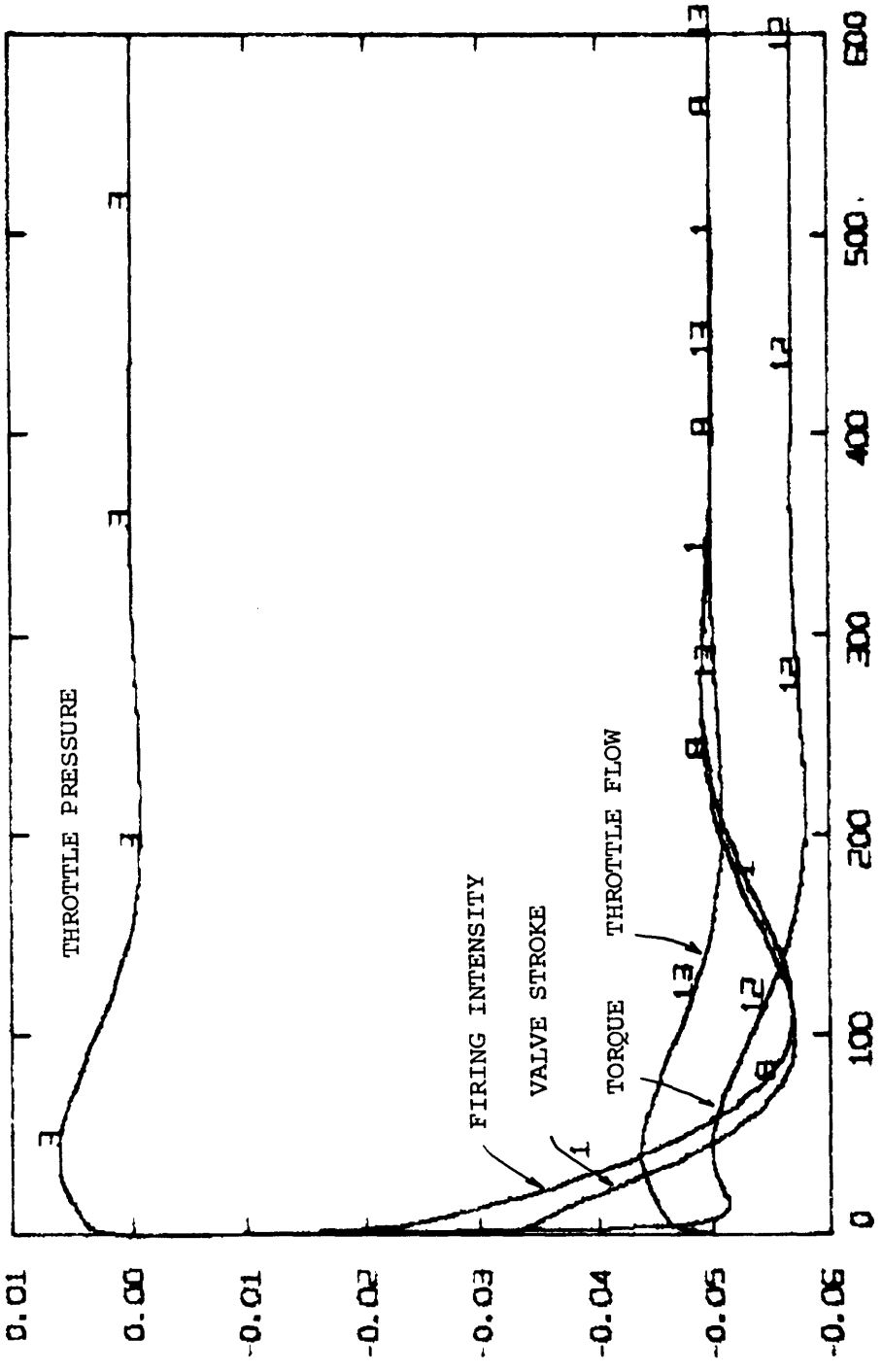

Fig. 27 Plant with PID Controller - 90% Load Level;
5% Step Decrease in Control Valve Opening
K = 4.5; T_i = 45; Td = 20

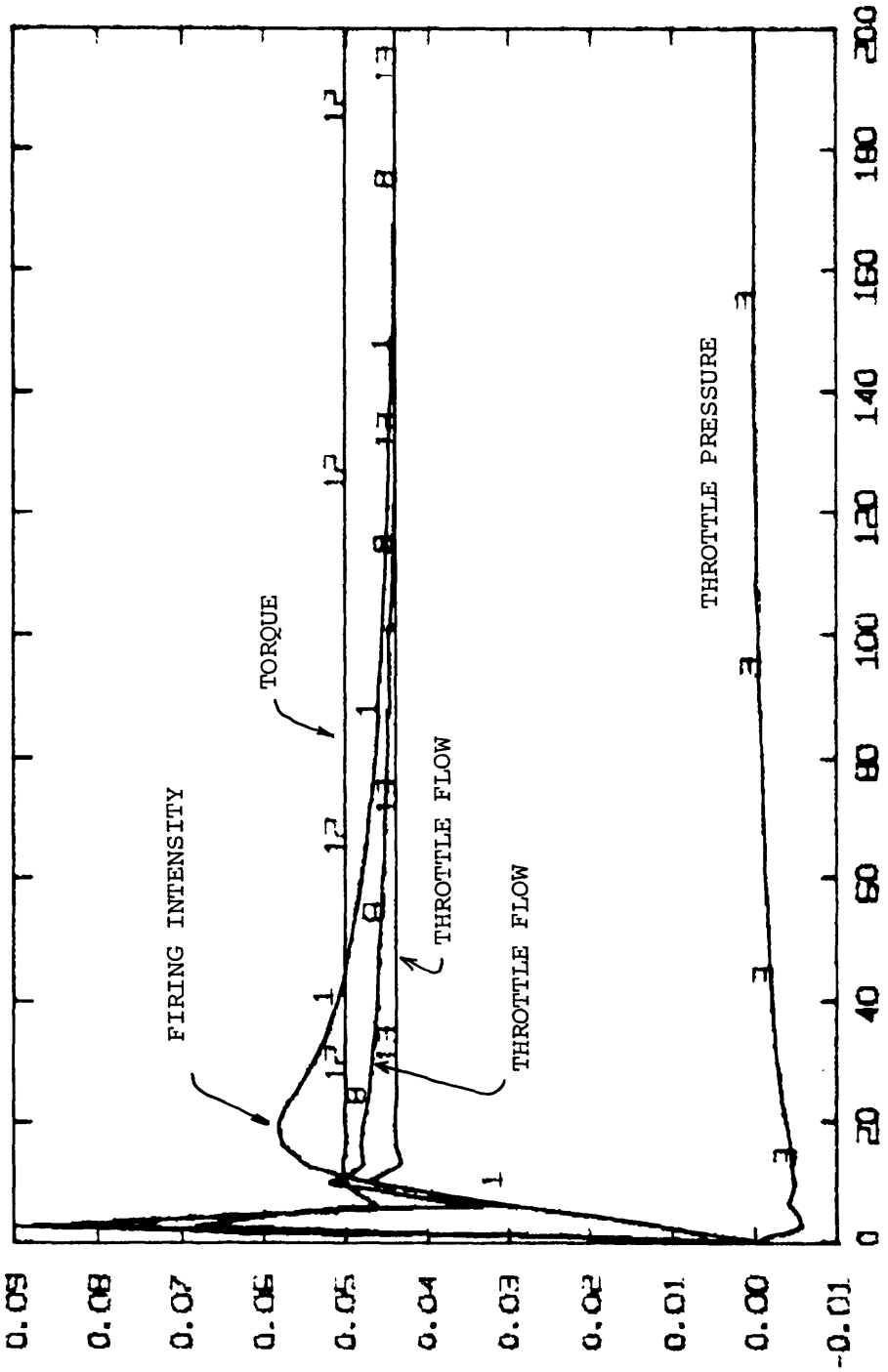

Fig. 28 Plant with Optimal Control - 90% Load Level;
5% Step in Load Demand; R = [0.25]

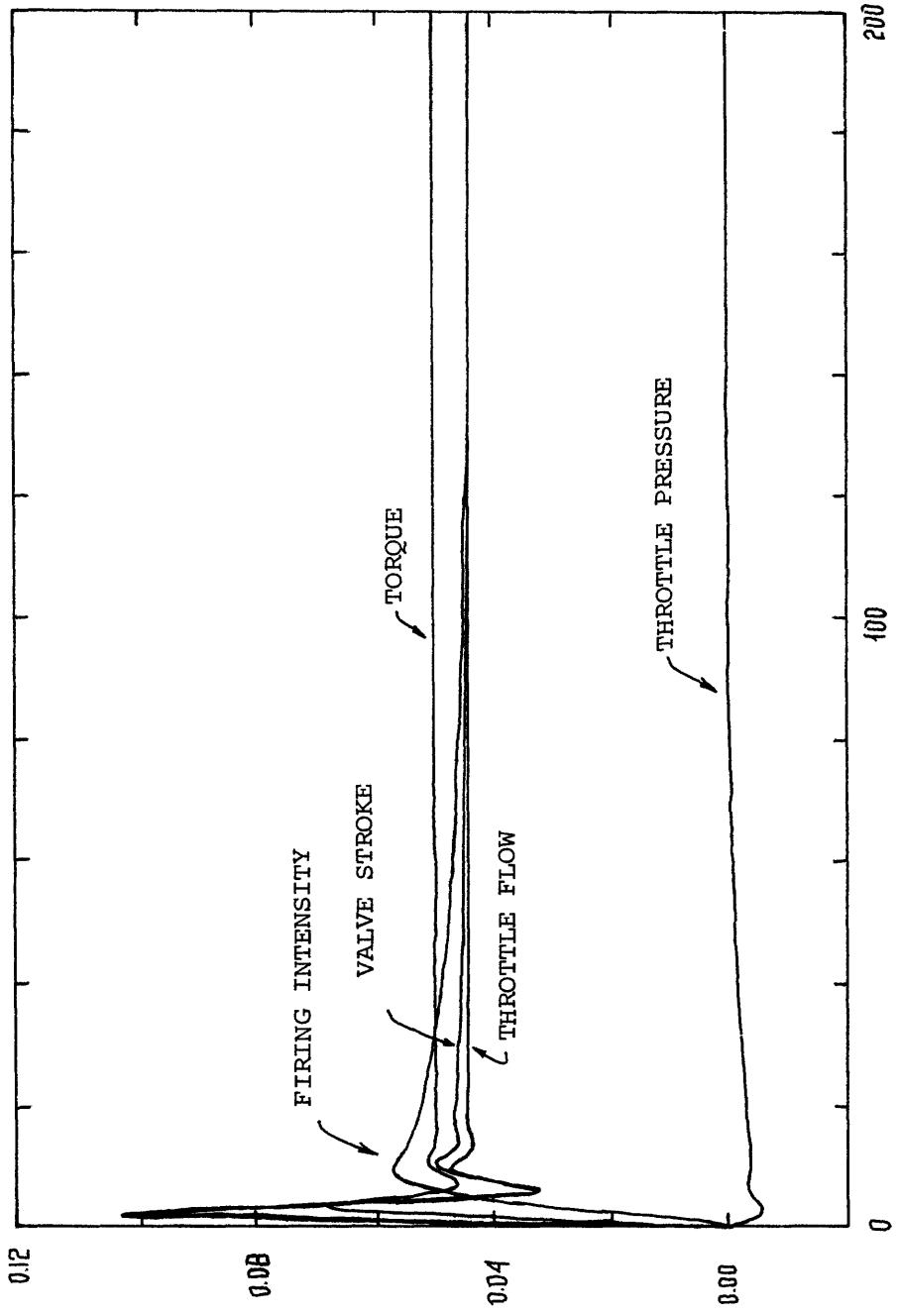

Fig. 29 Plant with Optimal Control - 90% Load Level;
5% Step in Load Demand; R = [4.0]

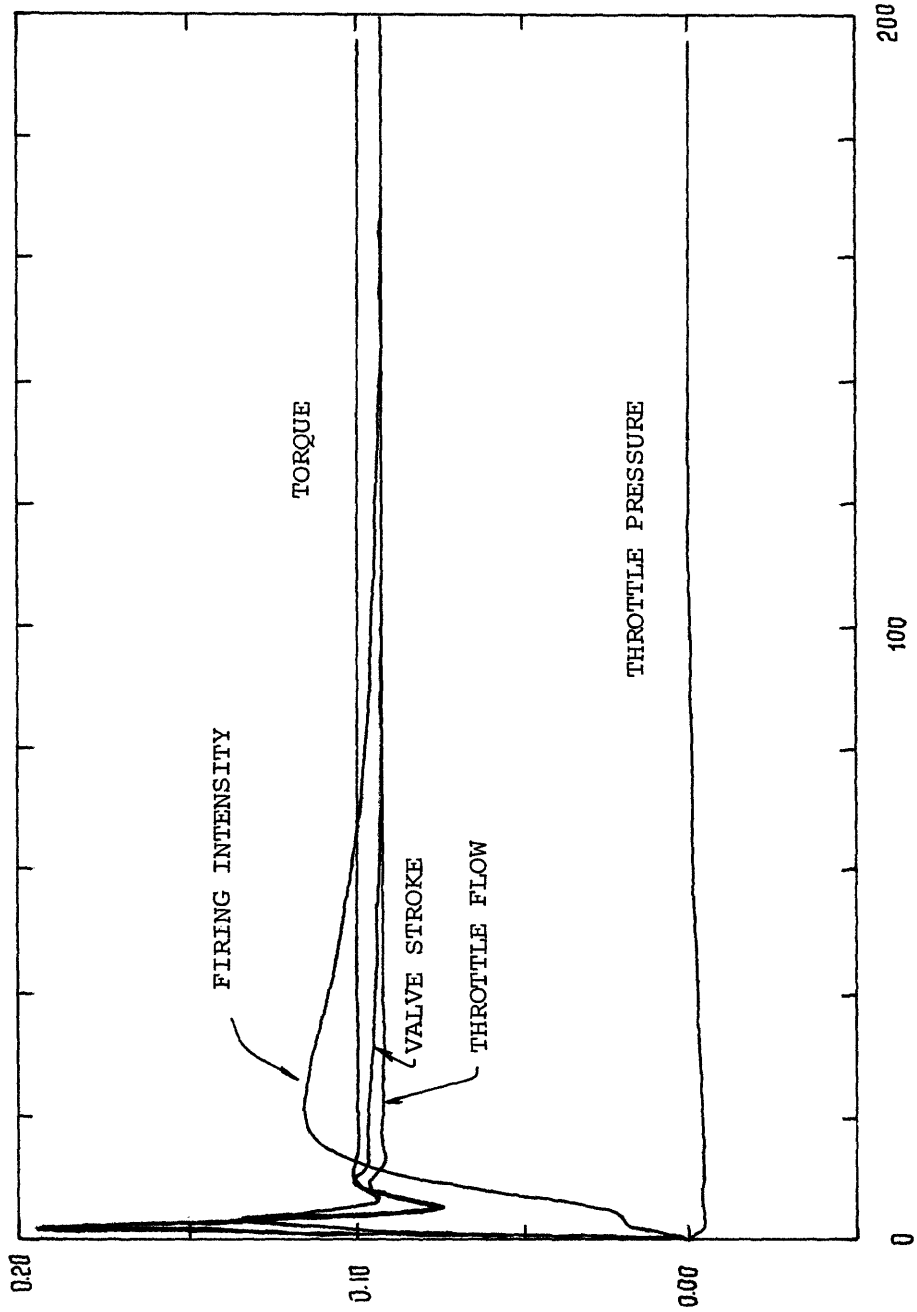

Fig. 30 Plant with Optimal Control - 60% Load Level;
10% Step in Load Demand; R = [4.0]

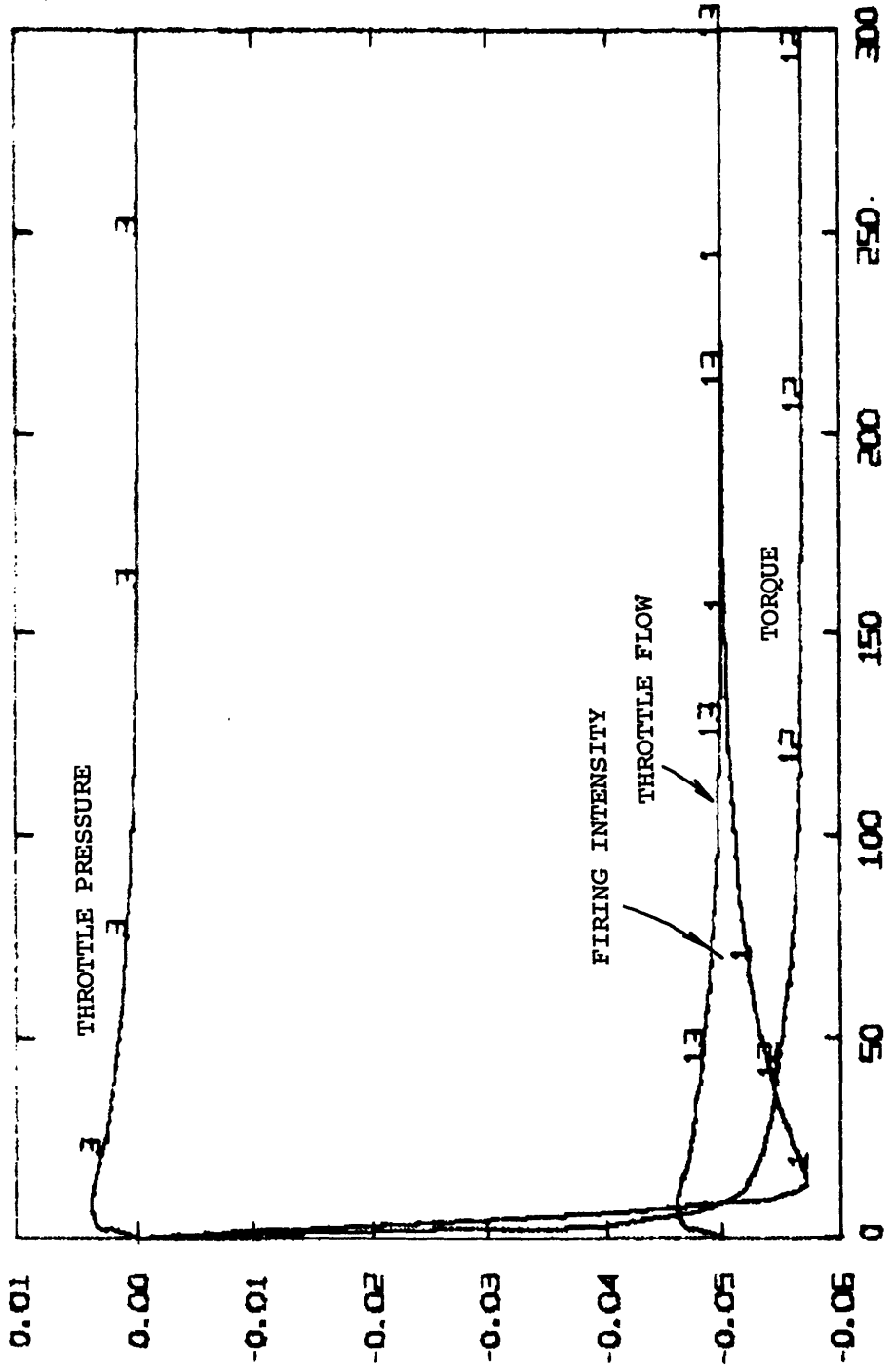

Fig. 31 Plant with Optimal Control - 90% Load Level;
5% Step Decrease in Control Valve Opening
R = [4.0]

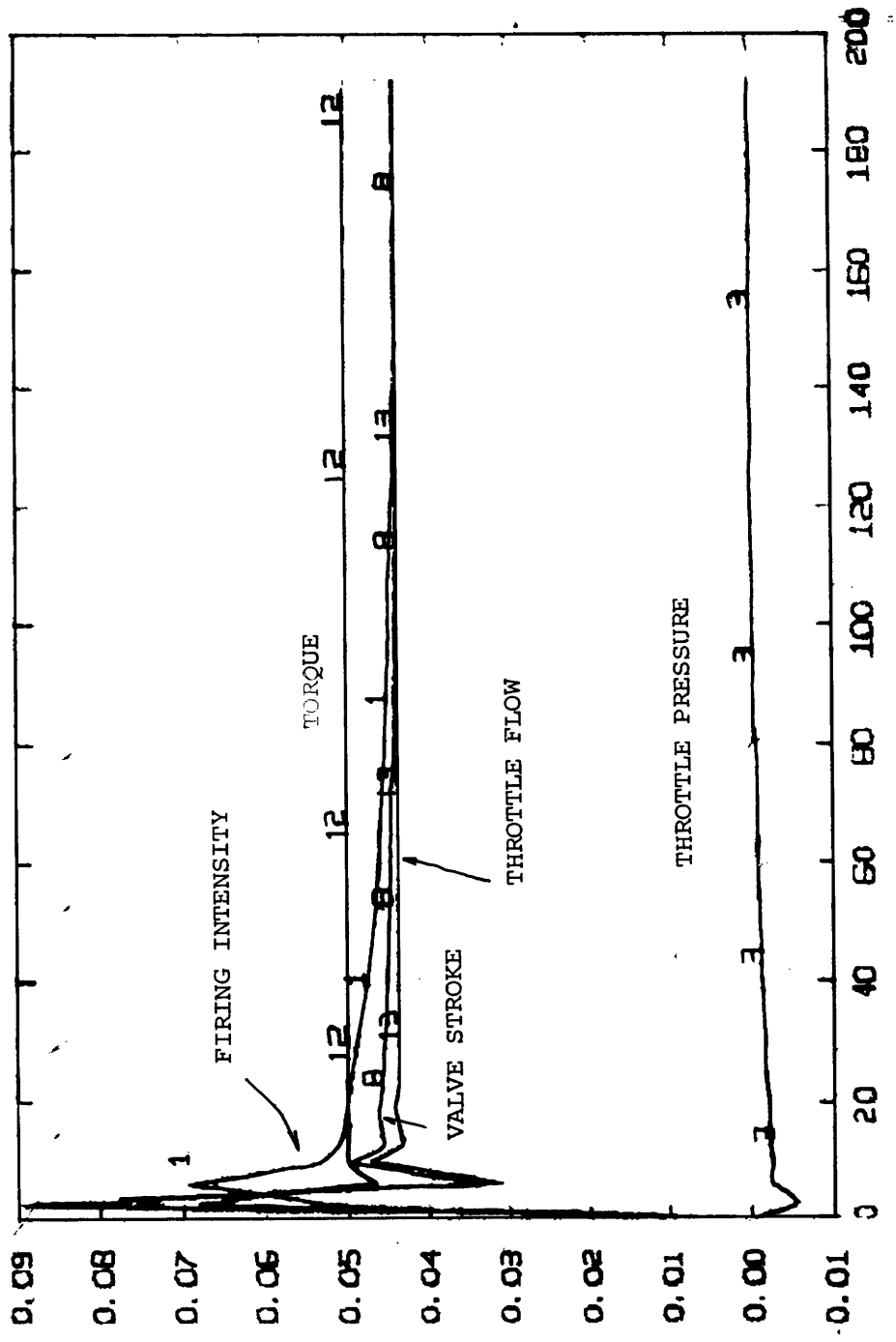

Fig. 32 Suboptimal Control - Suppressed Feedback of Steam Flows; 90% Load Level - 5% Step Increase in Load Demand; R = [4.0]

REFERENCES

1. Dolezal, R., Varcop, L., Process Dynamics, Elzevier, 1970.

2. Profos, R., "Dynamics of Pressure and Combustion Control in Steam Generators," Combustion, March, 1957.

3. Chien, K. L., et al., "Dynamic Analysis of a Boiler," ASME Transactions, Vol. 80, 1958.

4. Daniels, J. H., et al., "Dynamic Representation of a Large Boiler-Turbine Unit," ASME Paper No. 61-SA-69, 1961.

5. McDonald, J. P., Kwatny, H. G., "A Mathematical Model for Reheat Boiler-Turbine-Generator Systems," IEEE Paper 70 CP 221-PWR (1970).

6. Laubli, F. and Fenton F. H., Jr., "The Flexibility of the Supercritical Boiler as a Partner in Power System Design and Operation," Parts I and II, Trans. IEEE, PAS-90, No. 4 (July-August, 1971).

7. Anderson, P. M., "Mathematical Modeling of Boilers for Dynamic Stability Simulation," Power Plant Dynamics, Control and Testing Symposium, Knoxville, Tennessee, October 8-10, 1973.

8. Mika, H. S., "Pressure Ramping a Boiler by Automatic Throttle Pressure Set Point Control," Power Plant Dynamics, Control and Testing Symposium, Knoxville, Tennessee, October 8-10, 1973.

9. IEEE Working Group on Power Plant Response to Load Changes, "MW Response of Fossil Fueled Steam Units," IEEE Transac., PAS, March, 1967.

10. Anderson, J. H., et al., "Dynamic Control of a 200 MW Steam Generator," P.I.C.A., 1971.

11. IEEE Task Force on Overall Plant Response, "Dynamic Models for Steam and Hydro Turbines in Power System Studies," Paper T73 089-0, PES Winter Meeting, 1973.

12. Young, C. C., "Equipment and System Modeling for Large-Scale Stability Studies," Trans. IEEE, PAS-91, No. 1, Jan./Feb., 1972.

13. Shang, T. L., "Governing and Overspeed of Steam Turbines," M. S. Thesis, Course II, M.I.T., 1963.

14. Hedrick, J. K., "A Brief Review of Some Deterministic Linear-Quadratic-Regulator (LQR) Design Techniques," Appendix B, April 23, 1975.

15. Dorf, R. E., Modern Control Systems, Addison-Wesley, 1967.

16. Ogata, K., Modern Control Engineering, Prentice-Hall, 1970.

17. Anderson, J. H., Kwan, H. W., "Geometrical Approach to Reduction of Dynamical Systems," Proc. IEEE, Vol. 114, No. 7, July, 1967.

18. Fossil-Fuel Power Plant Dynamic Simulation of Boston Edison's Mystic No. 4 Unit, Mitre Corp., Bedford, Mass., 1975.

19. Keenan, J. H. and Keyes, F. G., Thermodynamic Properties of Steam 1st Edition, Wiley, 1967.

APPENDIX I - ACCUMULATION CHARACTERISTIC OF THE BOILER [1]

Consider a simplified fire tube boiler (evaporator) represented in Fig. 33, where

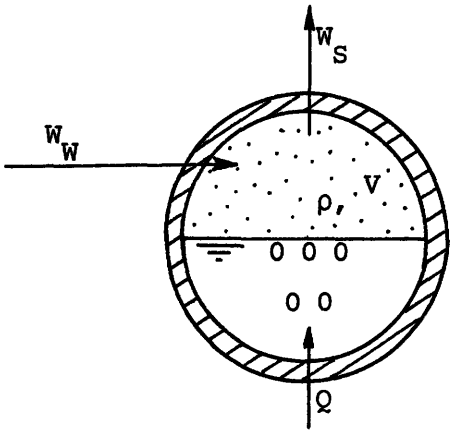

Fig. 33 Fire Tube Boiler Drum

W_W = feedwater inflow

W_{SH} = steam consumption

ρ = density of saturated steam

V_W = total volume of water in boiler

W_V = virtual steam production

$\dot{m}$ = rate of change of amount of steam in steam space

p_B = boiler pressure

From continuity:

$$\dot{m} = W_V - W_{SH} \tag{I-1}$$

If pressure changes at rate $\dot{p}_B$, the boiler stores or releases the following amount of energy, depending upon the sign of p:

$$\dot{Q}_a = \left(m_W \frac{\partial h}{\partial p_B} + m_E C_E \frac{\partial \theta}{\partial p_B}\right) \dot{p}_B \tag{I-2}$$

where

m_W = mass of water in evaporator

m_E = mass of metal in evaporator

C_E = specific heat of metal

h = enthalpy of water in evaporator

θ = saturated steam temperature

If r represents the heat of evaporation at the drum mean conditions, then the additional steam delivery due to heat released from the boiler storage is

$$W_{r1} = \frac{1}{r} \dot{Q}_a \quad . \tag{I-3}$$

However, there is another contribution from the expansion or contraction of steam bubbles present in the boiler water which must be taken into account:

$$W_{r2} = V_{WS} \frac{\partial \rho}{\partial p_B} \dot{p}_B \quad , \tag{I-4}$$

where V_{WS} is the total volume of steam bubbles dispersed in the water space.

Thus,

$$W_{SH} = W_V + W_{r1} + W_{r2} \quad . \tag{I-5}$$

In linearized form about a certain operating point, it can be written:

$$[\frac{1}{r}(m_W \frac{\partial h}{\partial p_B} + M_E C_E \frac{\partial \theta}{\partial p_B}) + V_{WS} \frac{\partial \rho}{\partial p_B}] \dot{\Delta p}_B = \Delta W_V - \Delta W_{SH} \quad . \tag{I-6}$$

Designating the expression between brackets by K_V and reducing to per-unit incremental value, we have

$$K_V \bar{p}_B \dot{p}_B = \bar{W}_V (W_V - W_{SH}) \tag{I-7}$$

where
$$p_B = \frac{\Delta p_B}{\bar{p}_B} = \frac{\text{pressure deviation}}{\text{steady-state pressure}} \tag{I-8}$$

$$W = \frac{\Delta W}{\bar{W}_V} = \frac{\text{flow deviation}}{\text{steady-state steam flow}} \quad . \tag{I-9}$$

Thus,

$$\underbrace{K_V \frac{\bar{p}_B}{\bar{W}_V}}_{T_V} \dot{p}_B = W_V - W_{SH} \tag{I-10}$$

where

T_V = time constant associated with the energy storage capacity of boiler

For a drum-type boiler the same expression (I-6) is valid, where m_E represents the mass of metal in the water walls and drum. However, the drum presents an asymmetric accumulation characteristic. If steam pressure rises, there is no corresponding reduction of the steam production in the drum [1], as it is not directly heated. We neglected such asymmetric behavior by considering that the boiler metal mass represents only 30% of the total mass and that we are on the safe side with respect to control applications.

Besides the energy storage we must take into account the mass storage capacity of the drum steam space and superheater tubes. The following lumped-parameter system applies (Fig. 34):

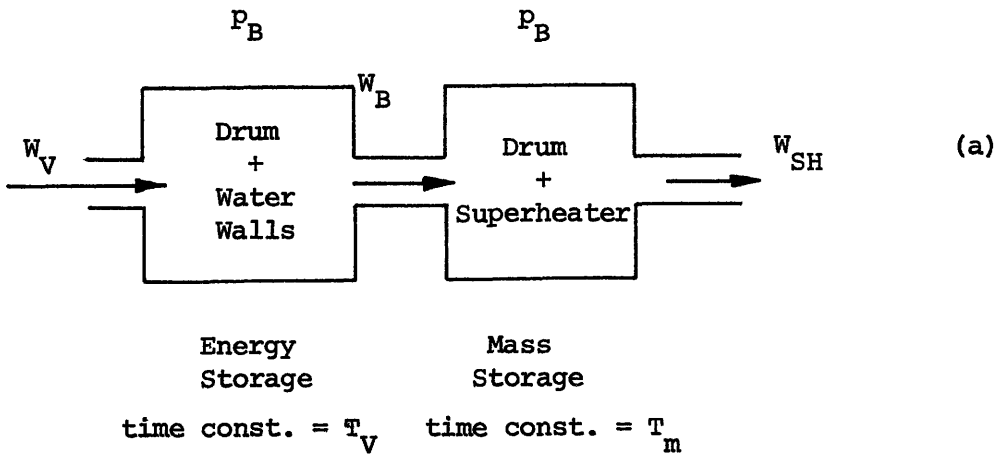

Fig. 34 Boiler Storage Capacity

Obviously one of the capacitances is not an independent energy storage element, since we are neglecting any resistance or inertance between them. The equations are as follows:

$$\dot{p}_B = \frac{1}{T_V} (W_V - W_B) \tag{I-11}$$

$$W_B - W_{SH} = T_m \dot{p}_B . \tag{I-12}$$

Or, combining (I-11) and (I-12):

$$\dot{p}_B = \frac{1}{T_R} (W_V - W_{SH}) \tag{I-13}$$

$$\text{where } T_R = T_V + T_m \ , \tag{I-14}$$

the total accumulation time constant of the boiler.

To estimate the value of T_m from design data, we use the following lumped-parameter model for pressure vessels for small deviations about a steady state operating point (Fig. 35).

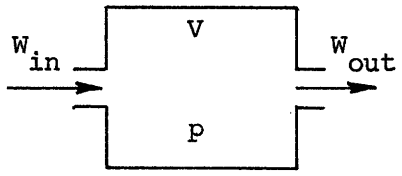

Fig. 35 Pressure Vessel

V = steam volume in vessel

p = steam pressure inside vessel

G = mass of steam inside vessel

W_{in}, W_{out} = steam flow into and out of the vessel

Continuity:

$$W_{in} - W_{out} = \dot{G} \qquad (\dot{G} = \frac{dG}{dt}) \tag{I-15}$$

$G = \frac{V}{v}$; v = specific volume of steam.

Assuming constant temperature:

$$\frac{1}{v} = \frac{1}{\bar{p}\,\bar{v}}\,p, \quad \text{where the bars indicate steady-state values} \tag{I-16}$$

$$\dot{G} = \frac{V}{\bar{p}\,\bar{v}}\,\dot{p} = W_{in} - W_{out} \tag{I-17}$$

$$\dot{p} = \frac{1}{T'}\,(W_{in} - W_{out}) \tag{I-18}$$

where $T' = \frac{V}{\bar{p}\,\bar{v}}$ is the time constant associated with mass storage in the vessel.

In scaled form we can write:

$$T = \frac{V}{\bar{p}\,\bar{v}} \cdot \frac{\bar{p}}{\bar{W}} \quad ,$$

where $\bar{W}$ represents the steady-state steam flow, $\bar{W} = \bar{W}_{in} = \bar{W}_{out}$

$$T = \frac{V}{\bar{v}\,\bar{w}} \quad \text{or, in equivalent form,}$$

$$T = \frac{\text{mass of steam in vessel}}{\text{steam flow through vessel}} \qquad \text{[seconds]}$$

Thus, for the boiler mass storage time, we obtain:

$$T_m = \frac{\text{mass of steam in steam space (lbm)}}{\text{Main steam flow (lbm/sec)}} \tag{I-19}$$

and for the main steam piping storage time:

$$T_p = \frac{\text{mass of steam in steam piping (lbm)}}{\text{main steam flow (lbm/sec)}}$$

APPENDIX II - COMPUTATION OF PARAMETERS

II(a) Boiler Parameters

Firing System

Typical values for the time constant T_F for oil-fired systems are in the range of 8 ∿ 10 seconds. The correct data can be obtained from test data for existing plants. We chose the value 10 seconds based on the Mystic No. 4 simulation model.

Accumulation Capacity (See Appendix I)

From Boston Edison Mystic No. 4 simulation model, we obtained the following basic data:

m_E = 369000 lb (Drum + waterwalls)

C_E = 0.11 Btu/lb ^{o}F

V_W = 990 ft^3 (Drum + waterwalls)

Quality of steam (x): at 60% load level = 9.75%

at 90% load level = 17.9%

Drum pressure (p_B): at 60% load level = 1852 psia

at 90% load level = 1917 psia

The values of $\frac{\partial h}{\partial p_B}$, $\frac{\partial \theta}{\partial p_B}$, and $\frac{\partial \rho}{\partial p_B}$ were estimated from steam tables [19] and are practically the same for both load levels:

$$\frac{\partial h}{\partial p_B} = 0.117 \ \frac{\text{Btu/lb}}{\text{psia}}$$

$$\frac{\partial \theta}{\partial p_B} = 0.074 \ ^{o}\text{F/psia}$$

$$\frac{\partial \rho}{\partial p_B} = 3.6 \times 10^{-3} \ \frac{\text{lbm/ft}^3}{\text{psia}} \quad .$$

The ratio between water and steam content in the water space is calculated as follows:

$$x = \text{Quality of Steam} = \frac{\text{mass of steam}}{\text{mass of water + mass of steam}}$$

$$x = \frac{V_S \rho_S}{V'_W \rho_W + V_S \rho_S}$$

$$\frac{V_S}{V'_W} = \frac{x}{1 - x} \frac{\rho_W}{\rho_S}$$

Considering $V_S + V_S + V'_W = 1$ (100%)

$$\left(\frac{V_S}{V'_W} + 1\right) V'_W = 1$$

$$V'_W = \frac{1}{\frac{x}{1 - x} \frac{\rho_W}{\rho_S} + 1} \quad \text{(per-unit of total volume)} .$$

The values of ρ_W, ρ_S, and r were obtained from steam tables as follows:

Load Level	60%	90%
ρ_S (lbm/ft^3)	4.762	5.008
ρ_W (lbm/ft^3)	40.0	39.53
r (Btu/lb)	491.	479.

The result of calculations are:

Load Level	60%	90%
$\frac{V_S}{V'_W}$	0.91	1.72
V'_W(per-unit)	0.52	0.37

The resultant steam volume and water mass (m) in the water space are as follows:

Load Level	60%	90%
Steam volume V_{WS} (ft^3)	475	622
Mass of water in (lbm)	20680	14545

Applying the equation (I-6) derived in Appendix I, we found for the time constant T_V:

T_V = 90 sec. at 60% load level

T_V = 176 sec. at 90% load level.

From Mystic No. 4 simulation model, we obtained the additional data:

Steam space in drum: 467 ft^3

Superheater storage volume: 2926 ft^3

Main steam pressure: 1820 psia

Main steam temperature: 1000 ^oF

Main steam flow: 136.4 lbm/sec. at 60% level

242. lbm/sec. at 90% level

The following steam space storage time was computed through the equation (I-19) in Appendix I:

Load Level	60%	90%
T_m (sec)	66	37
$T_R = T_V + T_m$ (sec)	242	127

Piping Storage and Pressure Drop

The main steam piping volume is 122 ft^3. From equation (I-20) in Appendix I, we obtain:

Load Level	60%	90%
T_p (sec)	3.0	1.5

The pressure drop coefficient is computed as follows:

$$K_{SH} = \left(\frac{\bar{W}_{SH}}{\bar{p}_B - \bar{p}_T}\right) \cdot \frac{\bar{p}_B}{\bar{W}_{SH}} = \frac{\bar{p}_B}{\bar{p}_B - \bar{p}_T}$$

Load Level	60%	90%
K_{SH} (dimensionless)	20	59

II(b) Turbine Parameters

Storage Time Constants

Typical values for the steam chest and cross-over time constants are available in the literature [11]. We chose the following values:

T_{CH} = 0.3 sec.

T_{CO} = 0.4 sec.

The dominant time constant in the turbine side corresponds to the reheater. We estimated its value based on Boston Edison Mystic No. 4 data and using the approximated method of computation of a steam vessel time constant presented in Appendix I:

Reheater volume (including piping) = 1256 ft^3.

Load Level	60%	90%
Inlet pressure (psia)	234	422
Outlet pressure (psia)	222	401
Average steam density (lbm/ft^3)	0.278	0.57
Steam flow (lbm/sec)	123	219
Reheater time T_{RH}	3.0	3.3

Power Fractions

For simplicity, we assumed the following typical values for power distribution through the turbine [11]:

Load Level	f_{HP}	f_{IP}	f_{LP}
60%	0.4	0.4	0.2
30%	0.3	0.4	0.3

The value of $\gamma = \frac{\partial h_I}{\partial p_1}$.

We estimated the value of $\frac{\partial h_I}{\partial p_1}$ from a Mollier's chart, assuming an enthalpy drop line as shown in Fig. 36:

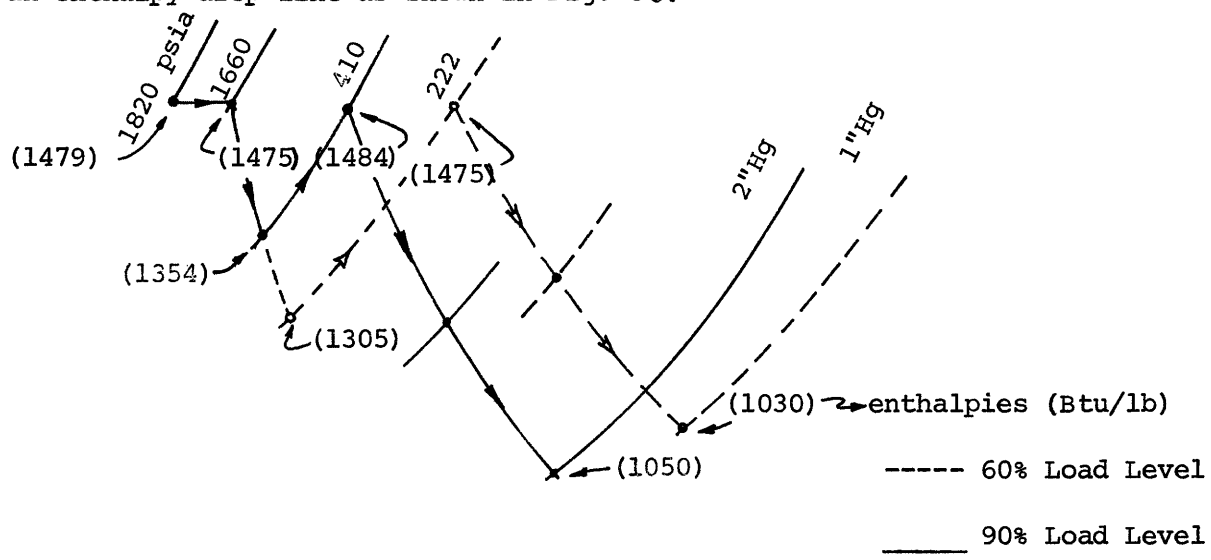

Fig. 36 Turbine Enthalpy Drop Lines

From the chart we can estimate the new expansion lines for a change in the pressure p_1. We tabulate the results as follows:

Load Level	60%	90%
Total enthalpy drop (Btu/lb)	616	555
H.P. drop at 1660 psia (Btu/lb)	171	125
H.P. drop at 1500 psia (Btu/lb)	168	120
$\Delta h/\Delta p_1$ (Btu/lb psia)	0.0188	0.0313
γ (normalized)	0.20	0.46

The new values at p_1 = 1500 psia were obtained assuming a parallel expansion line to that corresponding to p_1 = 1660 psia, which is approximately valid for small changes.

APPENDIX III - PID CONTROLLER EQUATIONS

The PID controller is of the form of Equation (46) whose equivalent frequency domain form is as presented below:

$$\frac{C_F(s)}{p_e(s)} = K\left(1 + \frac{1}{T_i s} + T_d s\right) \qquad \text{(III-1)}$$

where C_F = Firing setting (controller douput);

p_e = Pressure error = $p_o - p_T$;

p_o = Pressure set point (= 0. in our case) .

Therefore:

$$\frac{C_F(s)}{p_e(s)} = \frac{K}{T_i}\left(\frac{1 + T_i s + T_i T_d s^2}{s}\right) \qquad \text{(III-2)}$$

or

$$\dot{C}_F = \frac{K}{T_i}\left(p_e + T_i \dot{p}_e + T_i T_d \ddot{p}_e\right) . \qquad \text{(III-3)}$$

But $$\dot{p}_e = -\dot{p}_T \text{ , and} \qquad \text{(III-4)}$$

$$\ddot{p}_e = -\ddot{p}_T . \qquad \text{(III-5)}$$

Thus $$\dot{C}_F = \frac{K}{T_i}\left(-p_T - T_i \dot{p}_T - T_i T_d \ddot{p}_T\right) . \qquad \text{(III-6)}$$

From equations (2) and (3):

$$\dot{p}_T = \frac{1}{T_p}\left[K_{SH}(p_B - p_T) - W_o\right] \qquad \text{(III-7)}$$

$$\ddot{p}_T = \frac{1}{T_p}\left[K_{SH}(\dot{p}_B - \dot{p}_T) - \dot{W}_o\right] , \qquad \text{(III-8)}$$

But from equation (6):

$$\dot{W}_o = \xi \dot{p}_T + \dot{z} + \beta \dot{W}_1 \qquad \text{(III-9)}$$

Combining the equations (III-6), (III-7), (III-8) and (III-9), we get:

$$\dot{C}_F = \frac{K}{T_i}\left[-\frac{\chi}{T_p}(\xi + K_{SH}) - 1 + \frac{T_i T_d}{T_p}\left(\frac{\beta\xi}{T_{CH}} - \frac{K_{SH}^2}{T_R}\right)\right] p_T +$$

$$+ \left(\frac{\chi}{T_p} + \frac{T_i T_d}{T_p}\frac{K_{SH}^2}{TR}\right) p_B - \left[\frac{\chi}{T_p} - \frac{T_i T_d}{T_p}\frac{(\beta - 1)}{T_{CH}}\right]\beta W_1 -$$

$$- \left[\frac{\chi}{T_p} + \frac{T_i T_d}{T_p}\left(\frac{1}{T_{SV}} - \frac{\beta}{T_{CH}}\right)\right] z + \frac{T_i T_d}{T_p T_{SV}}\left(\frac{K}{\delta}\right)(n_o - n) -$$

$$- \frac{T_i T_d}{T_p}\frac{K_{SH}}{T_R} F + p_o \qquad \text{(III-10)}$$

where

$$\chi = \frac{T_i T_d(\xi + k_{SH})}{T_p} - T_i \,. \qquad \text{(III-11)}$$

The above expression gives the rate of increase in firing setting as a function of the state variables.

A much simpler expression can be obtained if we consider separately the effects of the proportional, integral, and derivative terms as indicated in Fig. 37.

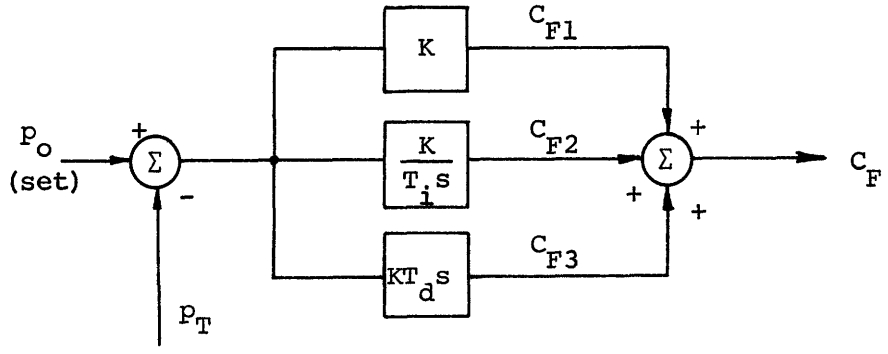

Fig. 37 PID Controller

Then

$$C_{F1} = - K p_T \tag{III-12}$$

$$C_{F2} = - \frac{K}{T_i} \int_o^+ p_T \, dt \tag{III-13}$$

$$C_{F3} = - KT_d \dot{p}_T \, , \tag{III-14}$$

and

$$C_F = C_{F1} + C_{F2} + C_{F3} \tag{III-15}$$

Both expressions (III-10) and (III-15) were used to obtain the plant response with PID controller. The last expression of equation (III-15) is a lot more convenient to use.

APPENDIX IV - OPTIMAL CONTROLLER PARAMETERS

The optimal controller gains (see Chapter III-3) depend on the choice of a suitable $\underline{Q}$ and R matrices. The $\underline{Q}$ matrix according to equation (60) was taken as

$$\begin{bmatrix} 1 & 0 & 0 & 0 & 0 & 0 & 0 & 0 \\ 0 & 0 & 0 & 0 & 0 & 0 & 0 & 0 \\ 0 & 0 & 11.11 & 0 & 0 & 0 & 0 & 0 \\ 0 & 0 & 0 & 0 & 0 & 0 & 0 & 0 \\ 0 & 0 & 0 & 0 & 0 & 0 & 0 & 0 \\ 0 & 0 & 0 & 0 & 0 & 0 & 0 & 0 \\ 0 & 0 & 0 & 0 & 0 & 0 & 0 & 0 \\ 0 & 0 & 0 & 0 & 0 & 0 & 0 & 0 \end{bmatrix}$$

where x_{1m}, the maximum allowance in firing rate was taken as 1.0 and x_{2m}, the maximum allowance in pressure was taken as 0.3 in per-unit values. These values can be justified by considering the pressure as the main controlled variable and thus with a greater weighting than the firing rate. The other variables, i.e., the boiler drum pressure and steam flow are functions of the firing rate and throttle pressure and so they are automatically limited. The turbine-side variables are also limited by the governor action. In view of these facts, only x_{1m} and x_{2m} were considered for optimal controller.

The optimal integral controller configuration is represented in Fig. 38.

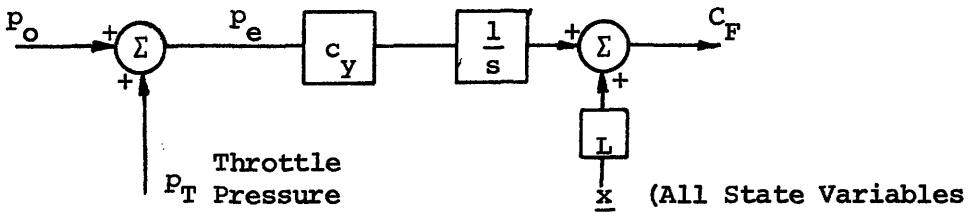

Fig. 38 Optimal Integral Controller

where $\underline{x}$ represents the state vector (8 x 1), and $\underline{L}$ and c_y are given by equation (73).

The Q matrix of equation (69) was established with the same x_{1m} and x_{2m} values as in the case of optimal controller without integral action. However, in this case another row and column were added with zero elements to take into account the new state variable u, of equation (63).

$\underline{L}$ and C_y matrices were computed for different values of R (input weighting matrix) and are listed in Table 7.

		Values of R (weight on input)		
		25.0	4.0	0.25
State Variable Feedback Coefficients (Gains)	L1	- 1,0304	- 0.6655	-0.3563
	L2	-66.79	-27.49	-7.426
	L3	- 0.912	- 0.374	- .1
	L4	- 0.1805	- 0.07405	-0.0198
	L5	- 1.192	- 0.4898	- 0.1312
	L6	- 0.06645	- 0.02717	- 0.00724
	L7	- 5.581	- 2.282	- 0.6079
	L8	0.0019	0.000768	0.0002
	L9	0.1	0.1	0.1
Int. Controller	CY	-16.66	- 6.667	- 1.667

Table 7 Optimal Integral Controller Gains

1. **Sample DYSYS Program - Plant with PID Controller**

```
      SUBROUTINE EQSIM
      DIMENSION A(9,9),Z(9,9),WR(9),WI(9)
      COMMON T,DT,Y(20),F(20),STIME,FTIME,NEWDT,IFWRT,N
     *,IPR,ICD,ICN,TNEXT,PNEXT,TBACK
      DATA KR,KW/8,5/
C     ENTER SCALING FACTORS
      DATA FN,PBN,PTN,W1N,W2N,W3N,ANN,ZN,CFN,AMN,W0N
     */.1,.01,.01,.1,.1,.1,.01,.1,.5,.1,.1/
      IF(NEWDT)1,2,3
1     CONTINUE
C     INITIALIZE ELEMENTS OF 'A' MATRIX
      DO 5 I=1,9
      DO 5 J=1,9
      A(I,J)=0.
5     CONTINUE
C     ASSIGNMENT OF VALUES FOR BOILER AND TURBINE PARAMETERS
C     BOILER PARAMETERS
      TF=10.
      TR=127.
      AKSH=20.
      TP=1.5
C     TURBINE AND GOVERNOR PARAMETERS
      CSI=1.
      BETA=0.
      GAMMA=.46
      THETA=0.
      GG=16.67
      TCH=.3
      TRH=3.3
      TCO=.4
      TA=10.
      TSV=.3
      FHP=.3
      FIP=.4
      FLP=.3
C     SET POINT VALUES
      AM0=.05
      AN0=0.
      P0=0.
C     PARAMETERS FOR PID CONTROLLER
      AK=Y(18)
      TI=45.
      TD=20.
C     EQUATIONS FOR PID CONTROLLER
      TID=TI*TD/TP
      CSIK=CSI+AKSH
      XI=(TID*CSIK-TI)/TP
      FT=AK/TI
      CPT=(-XI*CSIK-1.+TID*(BETA*CSI/TCH-AKSH*AKSH/TR))*FT
      CPB=(XI*AKSH+TID*AKSH*AKSH/TR )*FT
      CW1=(XI-TID*(BETA-1.)/TCH)*BETA*FT
      CZ=(XI+TID*(1./TSV-BETA/TCH))*FT
      CN0=(TID/TSV*GG)*FT
      CF =(TID*AKSH/TR )*FT
      CP0=FT
C     RESCALED MATRIX 'A' ELEMENTS
      A(1,1)=-1./TF
      A(1,9)=CFN/(FN*TF)
      A(2,1)=FN/(PBN*TR)
      A(2,2)=-AKSH/TR
```

```
      A(2,3)=AKSH/TR*PTN/PBN
      A(3,2)=AKSH/TP*PBN/PTN
      A(3,3)=-(AKSH+CSI)/TP
      A(3,4)=-BETA/TP *W1N/PTN
      A(3,8)=-ZN/(TP *PTN)
      A(4,3)=CSI/TCH*PTN/W1N
      A(4,4)=(BETA-1.)/TCH
      A(4,8)=ZN/(TCH*W1N)
      A(5,4)=W1N/(TRH*W2N)
      A(5,5)=-1./TRH
      A(6,5)=W2N/(TCO*W3N)
      A(6,6)=-1./TCO
      A(7,4)=(FHP*(1.+GAMMA))/TA*W1N/ANN
      A(7,5)=FIP/TA*W2N/ANN
      A(7,6)=FLP/TA*W3N/ANN
      ANM0=-AMN/(TA*ANN)
      A(7,7)=-THETA/TA
      ZN0=GG/TSV*ANN/ZN
      A(8,7)=-ZN0
      A(8,8)=-1./TSV
      A(9,1)=-CF/CFN*FN
      A(9,2)=CPB/CFN*PBN
      A(9,3)=CPT/CFN*PTN
      A(9,4)=-CW1/CFN*W1N
      A(9,7)=-CN0/CFN*ANN
      A(9,8)=-CZ/CFN*ZN
      CFN0=CN0/CFN*ANN
      CFP0=CP0/CFN*PTN
      W03=CSI/W0N*PTN
      W08=ZN/W0N
      W04=BETA/W0N*W1N
      AM4=FHP*(1.+GAMMA)/AMN*W1N
      AM5=FIP/AMN*W2N
      AM6=FLP/AMN*W3N
C     PRINT ORIGINAL COFFFICIENTS OF PID CONTROLLER EQUATION
      WRITE(KW,110) CPT,CPB,CW1,CZ,CN0,CF,CP0
110   FORMAT('0',     'CPT=',F10.2,5X,'CPB=',F10.2,5X,'CW1=',F10.3,5X,
     *'CZ=',F10.3,5X,'CN0=',F10.3,5X,' CF=',F10.4,5X,'CP0=',F10.5)
C     PRINT SCALED MATRIX 'A' AND COEFFICIENTS FOR TORQUF
C     ANDTHROTTLE FLOW EQUATIONS
      DO 10 I=1,9
10    WRITE(KW,200) (A(I,J),J=1,9)
200   FORMAT('0',9F12.5)
      WRITE(KW,220) ANM0,ZN0,CFN0,CFP0,W03,W08,W04,AM4,AM5,AM6
220   FORMAT(
     *'0','ANM0=',F12.5,5X,'ZN0=',F12.5,5X,'CNF0=',F12.5,5X,
     *'CFP0=',F12.5//'0','W03=',F12.5,5X,'W08=',F12.5,5X,'W04=',F12.5
     *//'0','AM4=',F12.5,5X,'AM5=',F12.5,5X,'AM6=',F12.5)
C     COMPUTE EIGENVALUES OF SYSTEM AND EIGENVECTORS
      CALL EISPAC(9,9,0,1,A,WR,WI,Z,IER,1111,1111,1)
3     CONTINUE
C     CALCULATION OF TURBINE TORQUE AND THROTTLE FLOW
      Y(12)=AM4*Y(4)+AM5*Y(5)+AM6*Y(6)
      Y(13)=W03*Y(3)+W04*Y(4)+W08*Y(8)
2     CONTINUE
C     SYSTEM OF DIFFERENTIAL EQUATIONS FOR DYSYS SIMULATION
      F(1)=A(1,1)*Y(1)+A(1,9)*Y(9)
      F(2)=A(2,1)*Y(1)+A(2,2)*Y(2)+A(2,3)*Y(3)
      F(3)=A(3,2)*Y(2)+A(3,3)*Y(3)+A(3,4)*Y(4)+A(3,8)*Y(8)
      F(4)=A(4,3)*Y(3)+A(4,4)*Y(4)+A(4,8)*Y(8)
```

```
 F(5)=A(5,4)*Y(4)+A(5,5)*Y(5)
 F(6)=A(6,5)*Y(5)+A(6,6)*Y(6)
 F(7)=A(7,4)*Y(4)+A(7,5)*Y(5)+A(7,6)*Y(6)+A(7,7)*Y(7)+ANM0*AM0
 F(8)=A(8,7)*Y(7)+A(8,8)*Y(8)+ZN0*AN0
 F(9)=A(9,1)*Y(1)+A(9,2)*Y(2)+A(9,3)*Y(3)+A(9,4)*Y(4)+A(9,7)*Y(7)+
*A(9,8)*Y(8)+CFN0*AN0+CFP0*P0
 RETURN
 END
```

2. Sample DYSYS Program - Plant with Optimal Controller

```
      SUBROUTINE EQSIM
      COMMON T,DT,Y(20),F(20),STIME,FTIME,NEWDT,IFWRT,N
     *,IPR,ICD,ICN,TNEXT,PNEXT,TBACK
      IF(NEWDT)1,2,3
1     CONTINUE
C     ASSIGNMENT OF VALUES FOR BOILER AND TURBINE PARAMETERS
C     BOILER PARAMETERS
      TF=10.
      TR=127.
      AKSH=20.
      TP=1.5
C     TURBINE AND GOVERNOR PARAMETERS
      CSI=1.
      BETA=0.
      GAMMA=.46
      THETA=0.
      GG=16.67
      TCH=.3
      TRH=3.3
      TCO=.4
      TA=10.
      TSV=.3
      FHP=.3
      FIP=.4
      FLP=.3
C     SET POINT VALUES
      AM0=.05
      AN0=0.
      P0=0.
C     FIRING INTENSITY AND VALVE STROKE LIMITERS
      ALIM=.11
      BLIM=-.5
      CLIM=.2
      DLIM=-1.
C     OPTIMAL CONTROLLER GAINS
      C1=-.6655
      C2=-27.49
      C3=-.374
      C4=-.07405
      C5=-.4898
      C6=-.02717
      C7=-2.282
      C8=.0007676
      C9=.1
      AK9=-6.666
3     CONTINUE
C     CALCULATION OF TURBINE TORQUE AND THROTTLE FLOW
      Y(12)=FHP*(1.+GAMMA)*Y(4)+FIP*Y(5)+FLP*Y(6)
      Y(13)=CSI*Y(3)+Y(8)+BETA*Y(4)
2     CONTINUE
C      SYSTEM OF DIFFERENTIAL EQUATIONS FOR DYSYS SIMULATION.
      IF(Y(1).GE.ALIM) Y(1)=ALIM
      IF(Y(1).LE.BLIM) Y(1)=BLIM
      IF(Y(8).GE. CLIM) Y(8)=CLIM
      IF(Y(8).LE. DLIM) Y(8)=DLIM
      F(1)=C1*Y(1)+C2*Y(2)+C3*Y(3)+C4*Y(4)+C5*Y(5)+C6*Y(6)+C7*Y(7)+
     *C8*Y(8)+C9*Y(9)
      F(2)=1./TR*(Y(1)-AKSH*(Y(2)-Y(3)))
      F(3)=1./TP*(AKSH*Y(2)-AKSH+CSI)*Y(3)-Y(8)-BETA*Y(4))
      F(4)=1./TCH*(Y(13)-Y(4))
```

```
F(5)=1./TRH*(Y(4)-Y(5))
F(6)=1./TCO*(Y(5)-Y(6))
F(7)=1./TA*(Y(12)-AMO-THETA*Y(7))
F(8)=1./TSV*(GG*(ANO-Y(7))-Y(8))
F(9)=AK9*Y(3)
RETURN
END
```

3. Sample Access Program - Computation of Optimal Integral Controller Gains

```
// XEQ ACCESS
INPUT AND PRINT MATRICES:
AB1(9,9) BB(9,1) HB(1,9) Q(9,9) RINV(1,1) ABHD1(9,9);
MATRIX AB1,
MATRIX BB,
0*0*0*0*0*0*0*0*1**
MATRIX HB,
0,0,1,0,0,0,0,0,0**
MATRIX Q,
1,0,0,0,0,0,0,0,0*
0,0,0,0,0,0,0,0,0*
0,0,11.11,0,0,0,0,0,0*
0,0,0,0,0,0,0,0,0*
0,0,0,0,0,0,0,0,0*
0,0,0,0,0,0,0,0,0*
0,0,0,0,0,0,0,0,0*
0,0,0,0,0,0,0,0,0*
0,0,0,0,0,0,0,0,0**
MATRIX RINV,
4.**
MATRIX ABHD1,
-.1,0,0,0,0,0,0,0,.1*
.007874,-.1575,.1575,0,0,0,0,0,0*
0,13.33,-14.00,0,0,0,0,-.6667,0*
0,0,3.333,-3.333,0,0,0,3.333,0*
0,0,0,.3030,-.3030,0,0,0,0*
0,0,0,0,2.5,-2.5,0,0,0*
0,0,0,.0438,.04,.03,0,0,0*
0,0,0,0,0,0,-55.56,-3.333,0*
0,0,1,0,0,0,0,0,0**
;
COMPUTE:
S1=MRA(AB1,BB,Q,RINV);
:T=-RINV*TRA(BB);
:G1=T*S1;
:LCY1=G1*INV(ABHD1);
// END
```